Title of Dissertation: GEOLOGIC STRUCTURES OF HIGHLY DEFORMED ROCKS AT OLIVER AND SNYDER HILLS, SOUTHEASTERN ADIRONDACKS, NEW YORK

AUTHOR: Youngdo Park

Read and Approved by:

Mary Louise Hill

Dr. M. L. Hill, Dept. of Geology, Temple University

Gene C. Ulmer

Dr. G. Ulmer, Dept. of Geology, Temple University

George H. Myer

Dr. G. Myer, Dept. of Geology, Temple University

Date submitted to Graduate Board:..

Accepted by Graduate Board of Temple University in partial fulfillment of the requirement for the degree of Master of Science.

Date:.. ....

(Dean of Graduate School)

GEOLOGIC STRUCTURES OF

HIGHLY DEFORMED ROCKS AT OLIVER AND SNYDER HILLS,

SOUTHEASTERN ADIRONDACKS, NEW YORK

A thesis
Submitted
in Partial Fulfillment
of the requirements for the Degree
MASTER OF SCIENCE

By
Youngdo Park
August, 1991

ABSTRACT

The study area is located at Snyder and Oliver Hills, Minerva, southeastern Adirondacks in New York State. The geologic setting of the study area is just south of the Anorthosite Suite of the Adirondack Massif. The rocks from the study area are granitic gneiss and amphibolite that were affected by high temperature metamorphism and deformation. The grade of metamorphism is interpreted from the mineral assemblage as relatively high P_{H2O} granulite facies metamorphism.

High temperature deformation is inferred since rock-forming minerals such as quartz, feldspar and calcite show microstructures related to plastic deformation. Strong and consistent rock fabrics are also found. Subhorizontal foliations are defined by compositional layering of mafic and felsic minerals. Subhorizontal east-west-trending lineations are defined by quartz ribbons and preferred orientation of mafic minerals. These conditions suggest subhorizontal ductile shear zone deformation in this area with the shear sense of hanging wall to the east or west.

To determine the shear sense, c-axis orientation from the quartz ribbon and grain shape orientation were measured. The pattern of the structural elements from these analyses is close to being symmetric rather than asymmetric, although the hanging wall to the west sense is slightly dominant. However, at an outcrop near the lithologic contact between the granitic gneiss and the amphibolite, a dragging fold of amphibolite is found. The shear sense from this outcrop is clearly hanging wall to the west. The hanging wall to the west shear sense and the symmetric pattern from the structural elements may suggest a close-to-coaxial but non-coaxial deformation or very large strain accumulation in this area.

Plastic deformation microstructures from the rock-forming minerals were carefully observed, since certain temperature conditions are required to form such textures. Microstructures found in this study include formation of quartz ribbons and quartz c-axis preferred orientation by basal <a> slip in quartz, feldspar subgrain boundaries by dislocation gliding, possibly cataclastic flow of feldspar grains, and deformation twins in calcite. The temperature conditions for these microstructures are plotted onto the regional cooling curve. These results may suggest that the deformation in this area lasted for a long period of time over a wide range of temperature conditions, although the nature of deformation, whether continuous or punctuated, is not exactly known.

Regionally, this study area is very highly deformed and not much literature is yet available in the areas adjacent to the study area. Hence it is hoped that the results of this study will aid as data base to future southern Adirondack studies.

ACKNOWLEDGEMENT

I would like to thank Dr. M. L. Hill, who introduced me to this project and gave me lots of motivation and help. Without her support, this thesis could not be done. Dr. G. Ulmer's criticism on the logic and the science of this manuscript was very beneficial. I am also indebted to Dr. G. Myer. He helped me in mineralogy, petrography, and interpretation of microstructures. Other faculty members including Drs. P. Goodwin, E. Anderson, D. Grandstaff and J. Adams are appreciated for their continuous encouragement while I was in graduate school.

Dr. R. Fakundiny at the New York State Geological Survey was of great help especially when I started this work, and I also thank the New York State Geological Survey for funding me during two summers. J. Ree introduced me to the literature that I used to calculate the grain shape fabric. R. Valentino and B. Bloomfield provided valuable suggestions.

CONTENTS

LIST OF TABLES

LIST OF FIGURES

I. INTRODUCTION

I-1. LOCATION OF FIELD AREA

The Adirondack massif is located in the northern part of New York State and is made up of high grade metamorphic rocks of amphibolite and granulite facies. The Anorthosite Suite occurs in the mid-eastern part of the massif. The field area of this study is located just south of the Anorthosite Suite (Figure I-1). The study area includes Oliver and Snyder Hills in the southeastern Adirondacks between longitude 73°55'W to 73°57'W, and latitude 43°47'N to 43°50'N. The nearest town to these hills is Olmstedville, 10 km. away from the Pottersville Exit of the New York State Thruway (Route I-87). The topography of the study area can be described as alternating cliffs and benches, surrounded by fault controlled north-south trending valleys (Figures I-2 & I-3). The cliffs are formed by granitic gneiss and the benches are formed by amphibolite.

The field work was done in the summer seasons of 1988 and 1989. Minerva Lake Beach Campsite provided a convenient site for base camp (location in Figure I-1).

I-2. GEOLOGIC SETTING

The Adirondack massif is largely composed of metamorphosed igneous plutons such as granite, syenite, anorthosite and gabbro with some metasedimentary rocks such as marble and metapelitic gneiss. Geological events can be grouped into

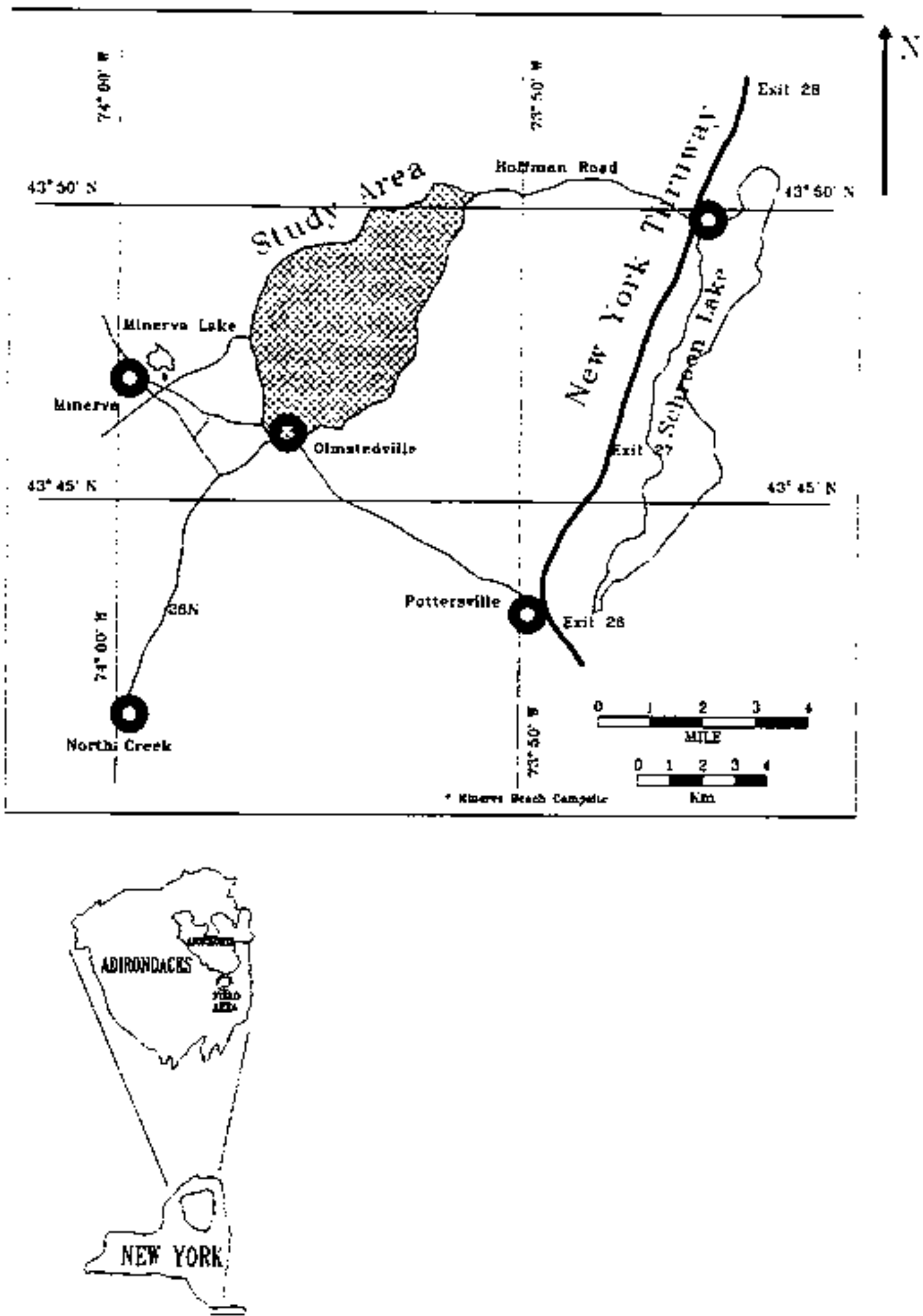

Figure I-1. Location of the study area.

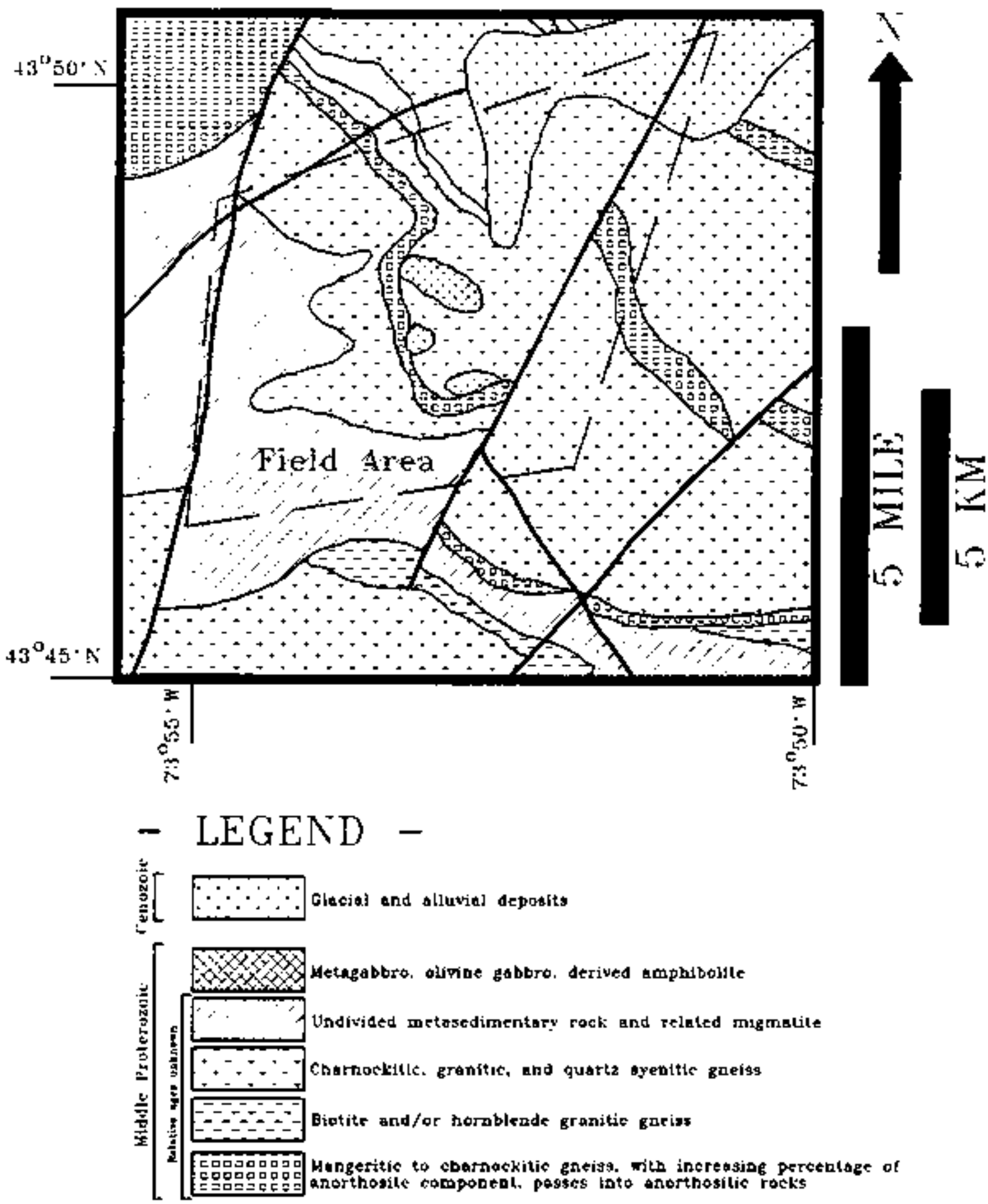

Figure I-2. Geologic map of the study area (Isachsen and Fisher, 1970). The study area is inside the dashed lines.

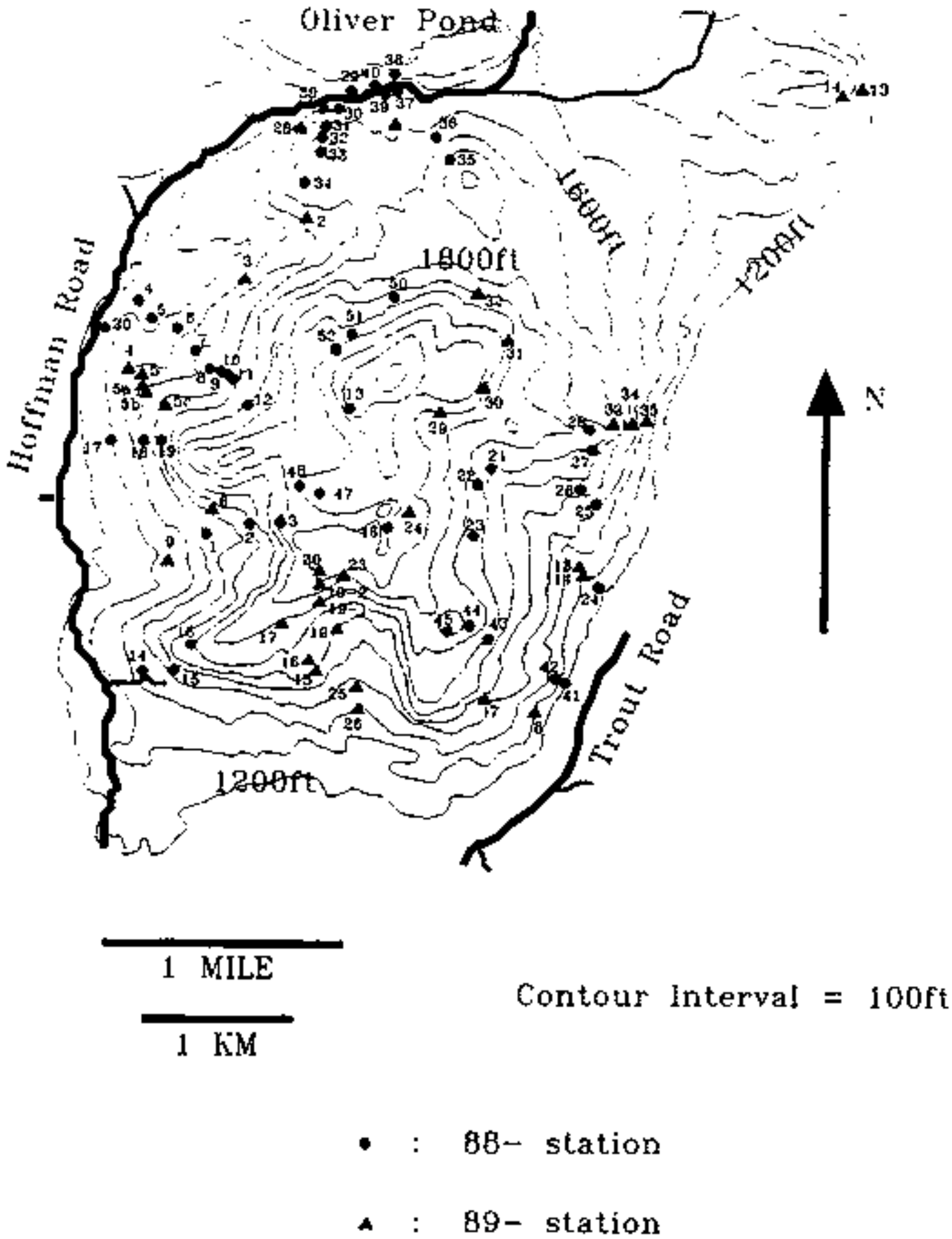

Figure I-3. Outcrop station map.

two episodes: (1) the anorthosite intrusion, (2) amphibolite and granulite facies metamorphism and high-temperature deformation.

In the mid-eastern part of the Adirondack massif occurs the Anorthosite Suite. There have been various models for the origin of the Anorthosite Suite (summarized in Best, 1982, pp. 548 - 549). In general, it is interpreted to have a magmatic origin. The emplacement is dated as around 1400 Ma and it is interpreted to have a different origin than the other rocks (Emslie, 1978).

Late Proterozoic high-grade regional metamorphism affected the rocks in the massif (Turner, 1981) and the accompanying and subsequent pervasive deformation made the origin and nature of the Adirondack massif difficult to interpret.

1-3. LITHOLOGY

The rock types of the study area as described in the New York State Geologic Map - Adirondack Sheet (compiled by Isachsen and Fisher, 1970) are metasedimentary rocks, charnockite gneiss, metagabbro and anorthosite (Figure 1-2). In this study, however, simple descriptive terminology is used for rock types because the lithologic nomenclature in the New York State Geologic Map was based on genetic interpretation chosen to describe the rocks in a regional scale.

The names chosen for map units in this manuscript are granitic gneiss and amphibolite interlayered with marble, which are respectively equivalent to charnockite and undivided metasedimentary rocks on the State Map (Table 1-1). With the outcrop map based on field work (Figures 1-3 and 1-4) and the chosen lithologic names (Table 1-1), the geologic map of this area was reconstructed (Figure 1-5).

Table I-1. Comparison of the lithologic unit nomenclature in the New York State Map and in this study.

<table>
<tr><th>Lithologic units of the New York State Geologic Map</th><th>Lithologic units used in this study</th></tr>
<tr><td>Glacial and alluvial deposits</td><td>Glacial and alluvial deposits</td></tr>
<tr><td>Metagabbro, olivine gabbro, and derived amphibolite</td><td rowspan="2">Amphibolite with interlayered marble</td></tr>
<tr><td>Undivided metasedimentary rock and related migmatite</td></tr>
<tr><td>Charnockitic, granitic, and quartz syenitic gneiss</td><td rowspan="2">Granitic gneiss</td></tr>
<tr><td>Mangeritic to charnockitic gneiss, with increasing percentage of anorthosite component, passes into anorthositic rocks</td></tr>
</table>

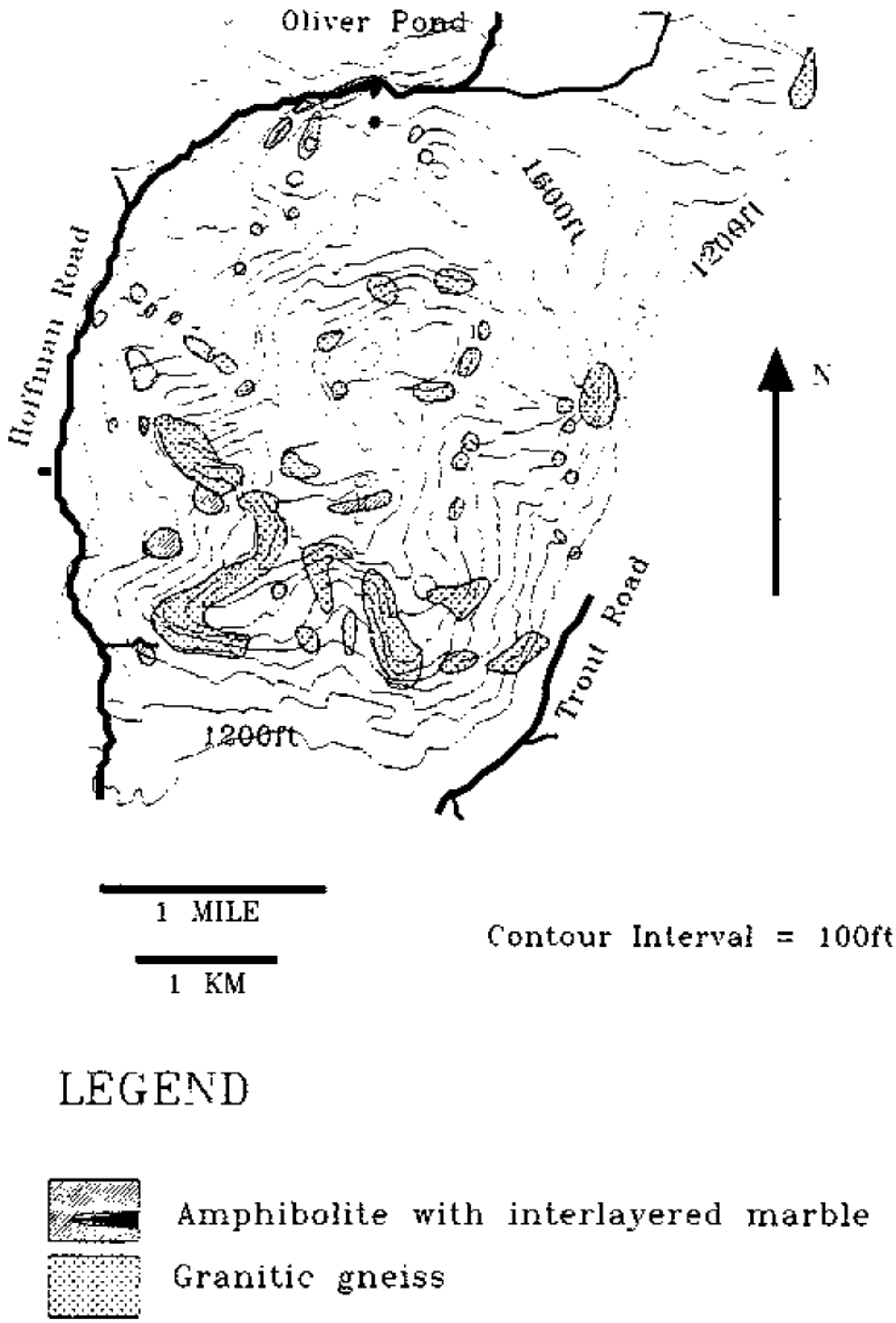

Figure I-4. Outcrop map of the study area.

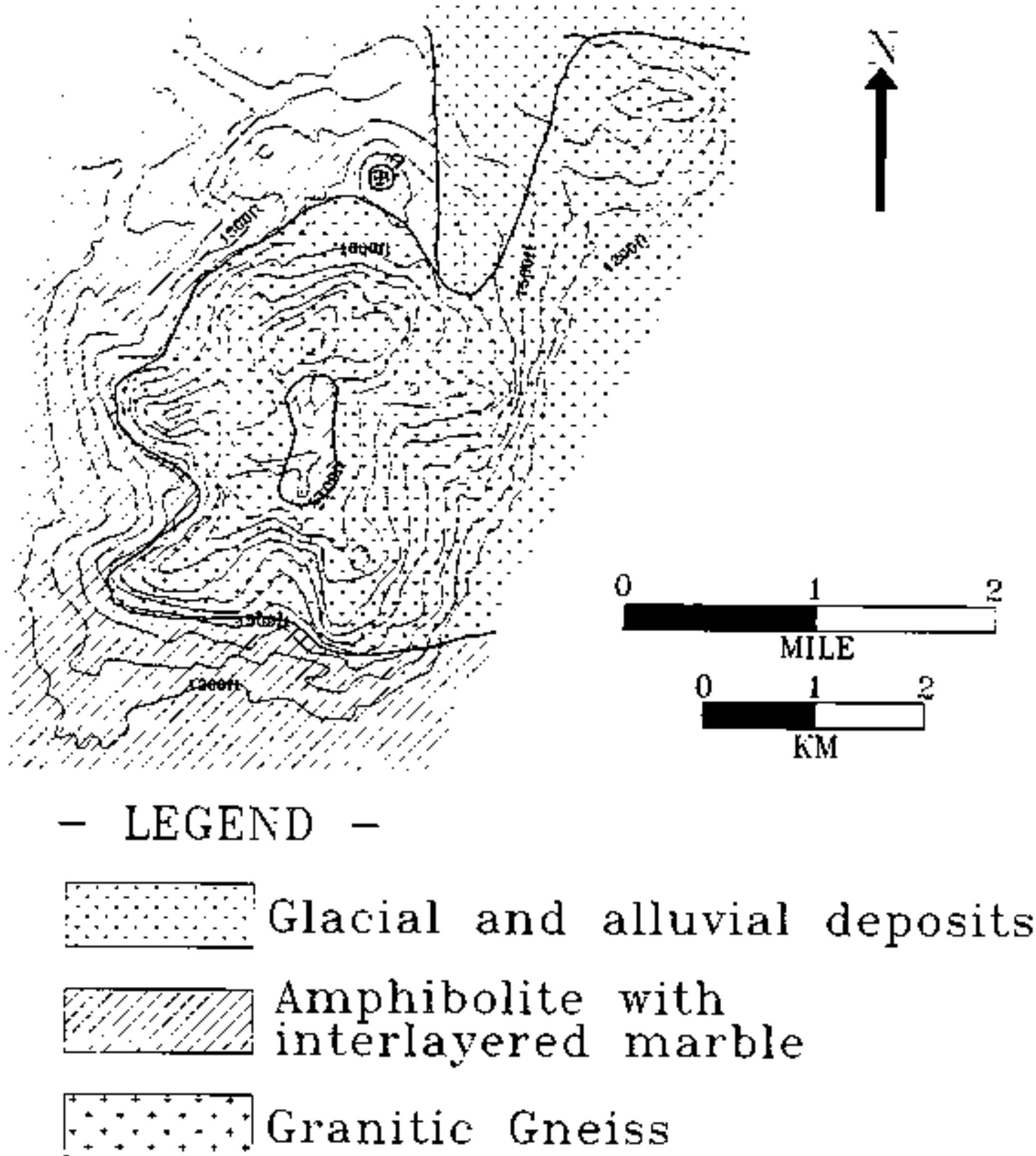

Figure I-5. Geologic map of the study area with the descriptive lithologic nomenclature based on the map in Figure I-4. Lithologic boundaries between the amphibolite and the granitic gneiss in the southern part of the study area are drawn after the New York State Geologic Map (Isachsen and Fisher, 1970).

Granitic Gneiss

The major minerals for this rock type are quartz and feldspar. The mafic minerals are garnet, amphibole, biotite and clinopyroxene. Charnockite, synonym for hypersthene granite (*sensu stricto*), as used in the State Map may not be an appropriate name because hypersthene is not usually found in this rock. A better name for this rock is quartzofeldspathic gneiss.

Amphibolite with interlayered marble

The major minerals for the amphibolite are amphibole, plagioclase, and orthopyroxene. The hand specimen color of this rock varies over a wide range depending on the amount of dark minerals (usually amphibole). The marble outcrops are found in the northern part of the field area.

I-4. SHEAR ZONE DEFORMATION

A ductile shear zone is defined as "*a zone with sub-parallel walls in which high deformations are localized. ...the strain variation* is *continuous across the zone such that, on the scale of a rock outcrop, no geometrical discontinuities can be seen.*" (Ramsay and Huber, 1983, p. 53). White and others (1980) emphasized strain softening* as the ductile shear zone formation mechanism because strain softening helps strain localization. Typical strain softening processes are grain size reduction by dynamic recrystallization and geometrical softening that will result in

* Glossary of terms is given in Appendix A.

fabric development. Therefore, the mylonites formed in a ductile shear zone are characterized by strong fabric and grain size reduction.

Strong planar and linear fabrics in the field, and microstructural evidence for plastic deformation such as subgrain boundaries and deformation twins are found. The structures suggest subhorizontal shear zone deformation, with hanging wall to the east or west movement. Kinematic data from the quartz c-axes fabric and S-C fabric analysis with the outcrop evidence constrain the sense of shear.

I-5. PURPOSE OF THE STUDY

When rocks are under a high temperature ductile deformation, changes in microstructures of minerals or in structures of rocks are expected. These structural changes are used to interpret the nature of deformation.

The purpose of this study is to document the structural changes and apply them to understand the nature of deformation in this area. Various plastic deformation microstructures of minerals and rock textures are used as a basis. From this, interpretations about the deformation are presented. They include shear sense, temperature conditions for the deformation, and dating the deformation using the regional cooling curve.

II. METHODOLOGY

II-1. FIELD METHODS

The base map used for geologic mapping is the Schroon Lake Quadrangle (1:62,500) of New York State. Eighty oriented samples were taken for structural and petrographic study. Localities and orientations of the samples are in Figure I-2 and Appendix B, respectively.

Garnet pressure shadows, rolling structures and fabric transposition were carefully examined during the field work to determine the sense of movement in the field area.

II-2. METHODS USED FOR LITHOLOGIC STUDY

Thin sections were cut perpendicular to foliation and parallel to lineation. The view point of thin sections in this study is generally looking from the north (Figure II-1).

Since the ductile shear zone deformation was very intensive and made the overall grain size very small, identification of minerals, especially K-feldspar, plagioclase and quartz, was difficult. Therefore, selective staining of these minerals on rock slabs (Bailey and Stevens, 1960) was done. Care was taken to avoid overstaining of plagioclase lamellae in the perthite by residual and mobile Ca ions which will occur if the sample stays too long in the hydrofluoric acid.

Modal mineralogy was determined by point counting. The error range of the point counting was determined after the statistical method of van der Plas and

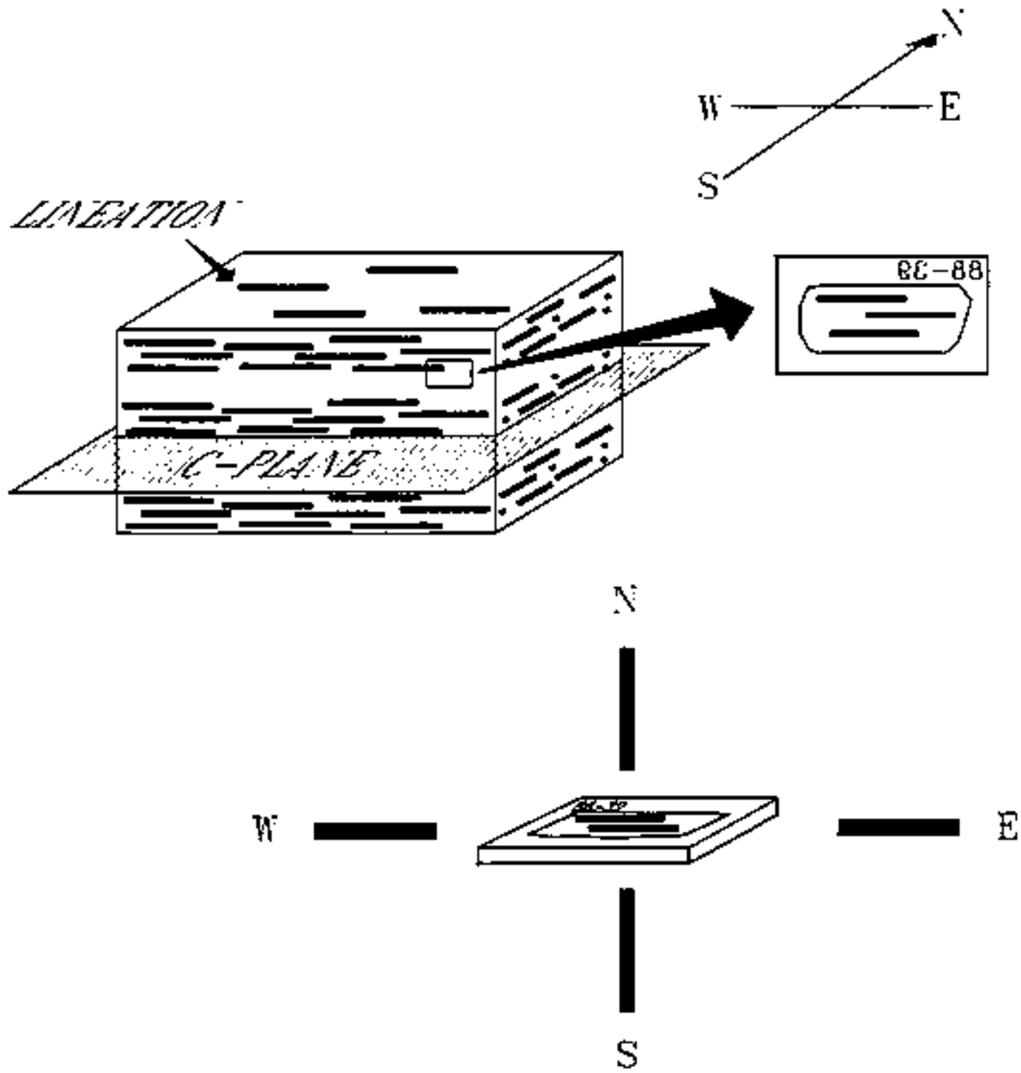

Figure II-1. Orientation of thin sections. Thin sections are made perpendicular to foliation and parallel to lineation. The view point is from the north.

Tobi (1965). An X-ray diffractometer (Model D-MAX/B by Rigaku) was used to determine the composition of mafic and opaque minerals.

II-3. METHODS FOR MEASURING THE C-AXES ORIENTATION OF QUARTZ

Quartz c-axis fabric (crystallographic preferred orientation pattern) analysis gives information about such things as major slip systems, whether the deformation is coaxial or non-coaxial, and sense of shear. The most widely used instruments to measure the c-axis orientation are the Universal Stage and the X-ray diffractometer with textural goniometer. In this section, a faster and simpler technique to measure the c-axis orientation on a regular (flat) stage microscope will be discussed.

During the observation of quartz ribbons from the granitic gneiss for this study, an abnormally high interference color from quartz was observed. This quartz is hereafter referred to as "*yellow Quartz*" (Figure II-2). There are two possible explanations for the yellow quartz. First, the value of the birefringence(δ) reaches a maximum (δ=0.009, first order "*straw yellow*" interference color) when the c-axis of quartz is parallel to the microscope stage. Second, since the abrasive hardness of a plane parallel to the c-axis may be greater than that of a subbasal plane, the real thickness of a section parallel to the c-axis is greater than that of one parallel to the subbasal plane (Figure II-3). Or, the combined effects of both explanations may be the cause for the abnormally high interference color. Yellow quartz is useful because it indicates that the c-axis is nearly parallel to the microscope stage.

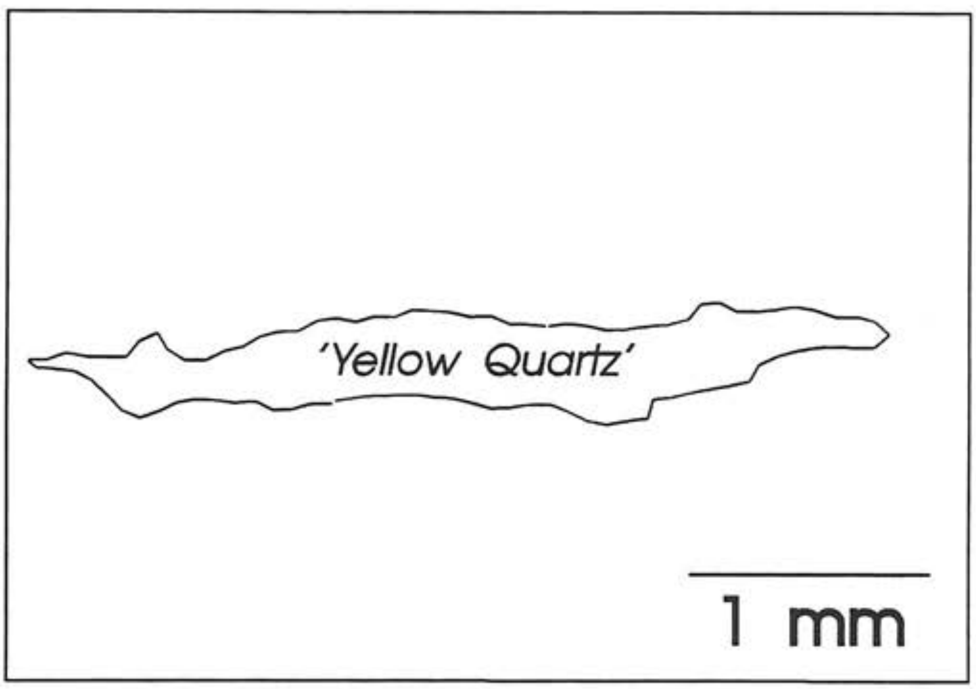

Figure II-2. Crossed polarized light photomicrograph of "yellow quartz" from the granitic gneiss. This abnormally high interference color is used to choose the quartz grains whose c-axes are nearly parallel to the stage of microscope.

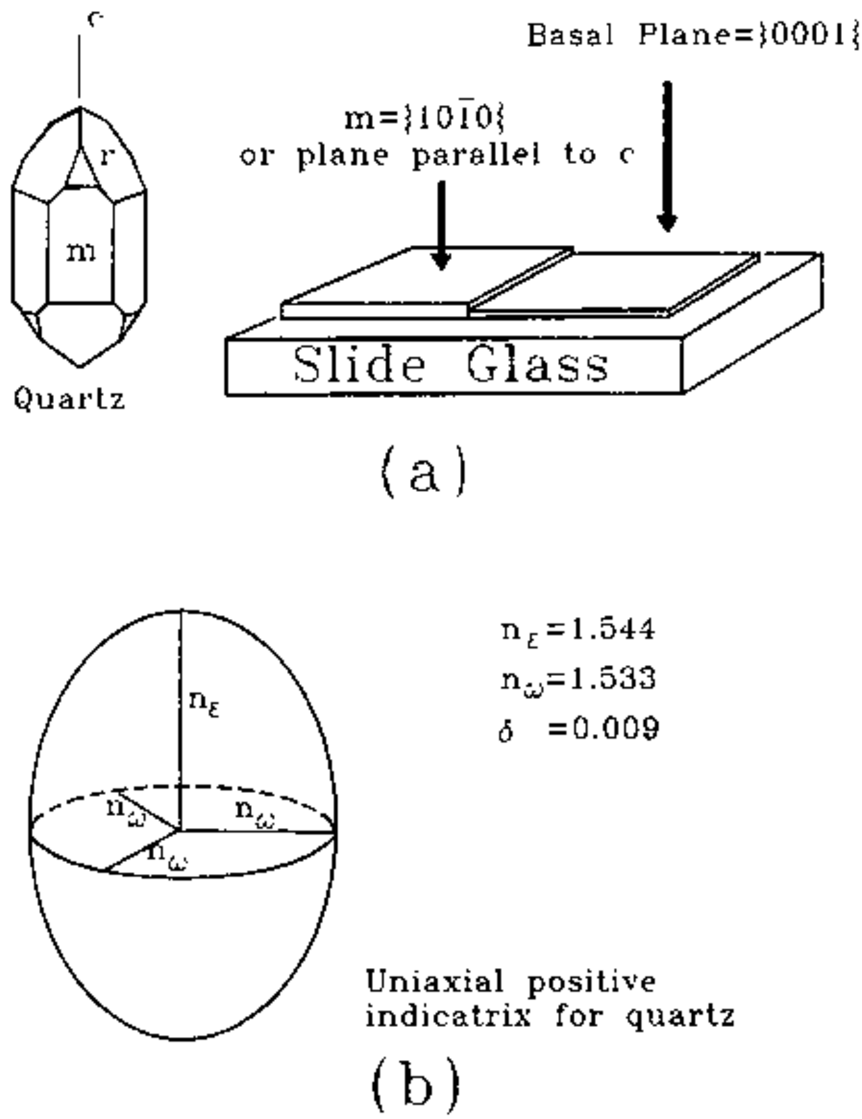

Figure II-3. Possible explanations for "yellow quartz". (a) Abrasive hardness of planes parallel to c-axis is greater than that of planes normal to c-axis. (b) The direction of the highest interference color is normal to c-axis.

Another noteworthy property of the quartz from the study area is that the crystals go to extinction when the subgrain boundaries are set parallel to the north-south or east-west cross hairs of the microscope, indicating that the subgrain boundaries are parallel to the c-axis. c-axis orientation, therefore, is either parallel to the north-south or east-west cross hair, and it is easy to distinguish one of these as the c-axis orientation using a gypsum plate. With a gypsum plate inserted at the extinction position, if the interference color increases after slight clockwise rotation of stage, then c-axis orientation is parallel to the north-south cross hair. On the other hand, c-axis orientation is parallel to the east-west cross hair if the interference color decreases after same rotation.

Combining the two assumptions, (1) yellow quartz indicates that the c-axis is nearly parallel to the microscope stage and (2) subgrain boundaries are parallel to the c-axis, it is possible to measure the c-axis of quartz on a flat stage, as long as these two features (yellow quartz and subgrain boundaries) are present. This technique was tested by looking at the interference figures; uniaxial flash figures confirmed the predicted crystallographic orientation.

The quartz c-axis fabric is plotted on a rose diagram instead of a stereonet because the angle of difference between the c-axis and the microscope stage cannot be measured precisely by this method. There is a possible range of 20 to 30 degrees in this angle, but the c-axis fabric plotted on a rose diagram is still valuable to determine the sense of shear in a non-coaxial deformation (Etchecopar, 1977). Plotting on a rose diagram and a stereonet is compared in Figure II-4.

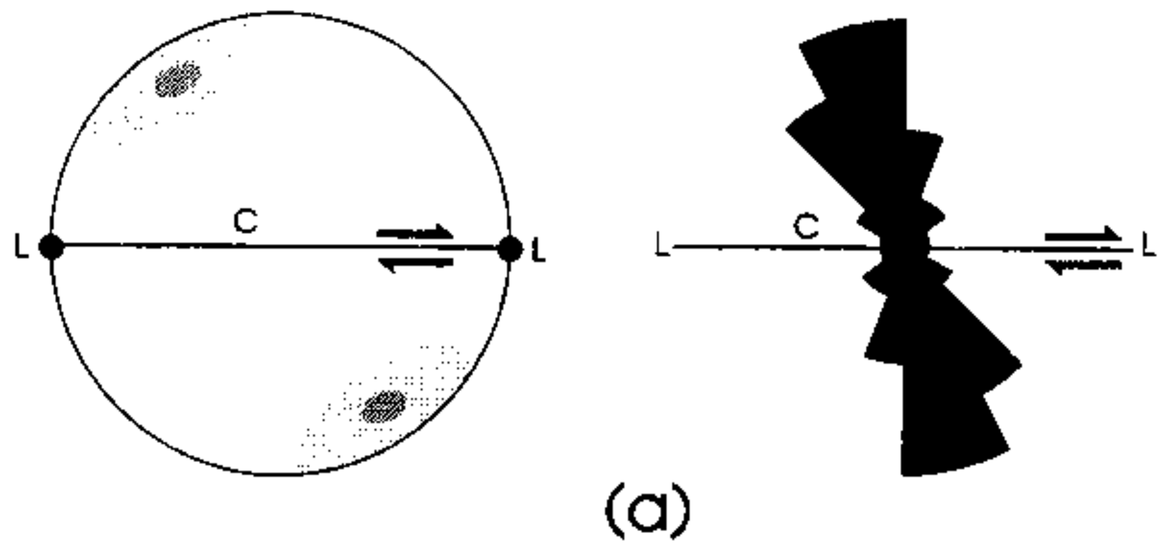

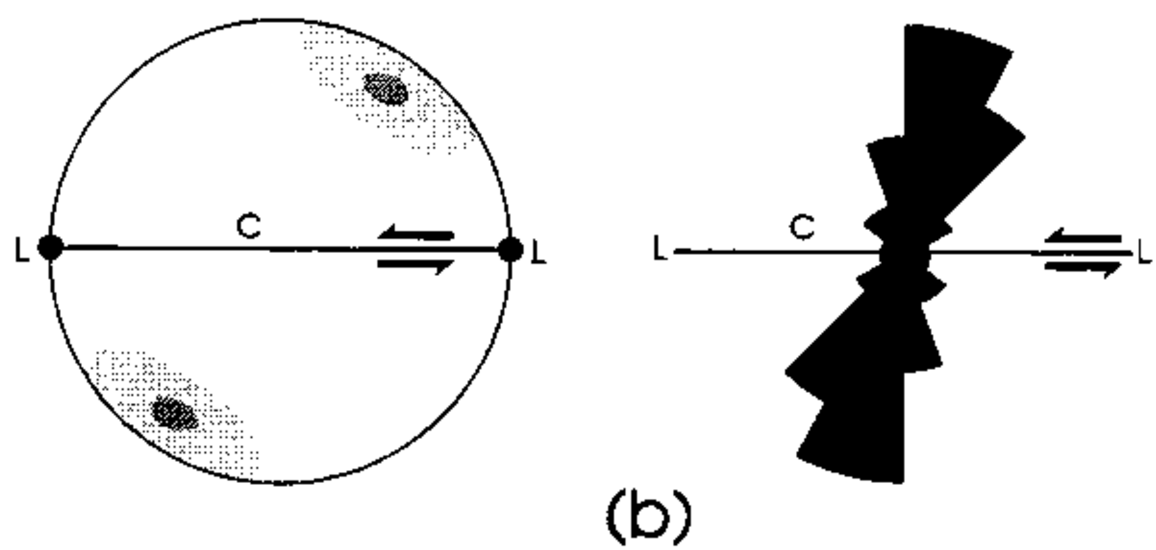

Figure II-4. Quartz c-axis pattern on a stereonet and a Rose diagram when the major working slip plane is {0001}. In this study, a Rose diagram is used because c-axis plunge is not measured. (a) c-axis pattern after dextral simple shearing. (b) c-axis pattern after sinistral simple shearing.

II-4. METHODS FOR ORIENTING THE GRAIN SHAPE FABRIC

In the granitic gneiss from the field area, a quartz ribbon fabric which is oblique to the mafic mineral layering was observed (Figure II-5). The mafic mineral layering is assumed to be parallel to the shear zone boundary or the C-fabric because it is more consistent and stronger than the quartz ribbon fabric, and the quartz ribbon fabric is assumed to be equivalent to the S-fabric. Since the angle between the mafic mineral layering and the quartz ribbon is very small and also varying, it is not reliable to determine the sense of shear by rough estimation. A computer program, called "GBO" (grain boundary orientation calculation) was written to get the orientation of grain shape fabric (Figure II-6 and Appendix C). By doing separate digitizing on mafic minerals and quartz ribbons, their maximum orientation value (α) can be calculated, and these angular relationships are used to determine the sense of shear.

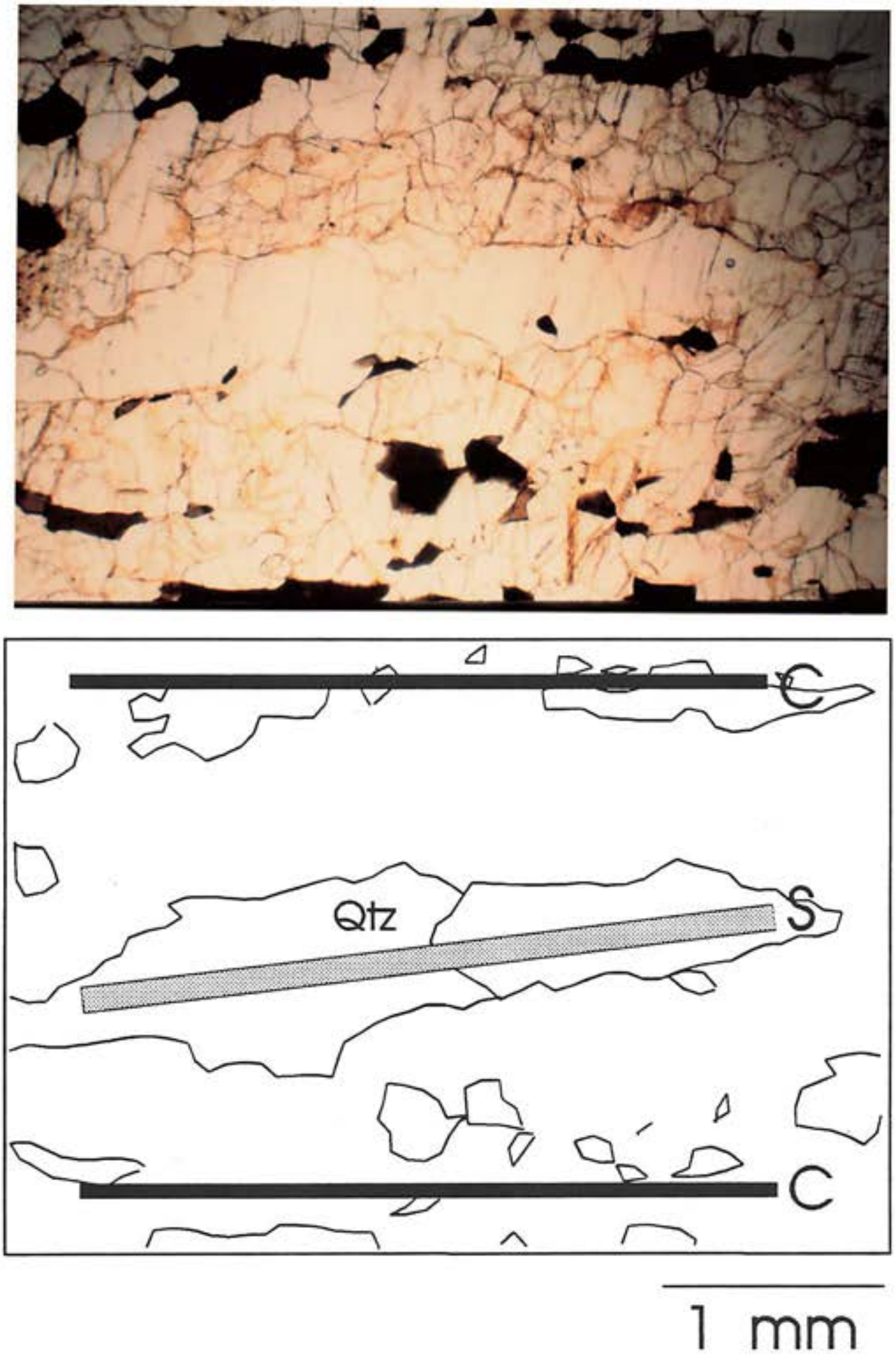

Figure II-5. Plane polarized light photomicrograph of S- and C- fabric from the granitic gneiss (viewed from the north). C-plane is defined by layering of mafic minerals and S-plane is defined by quartz (Qtz) shape fabric.

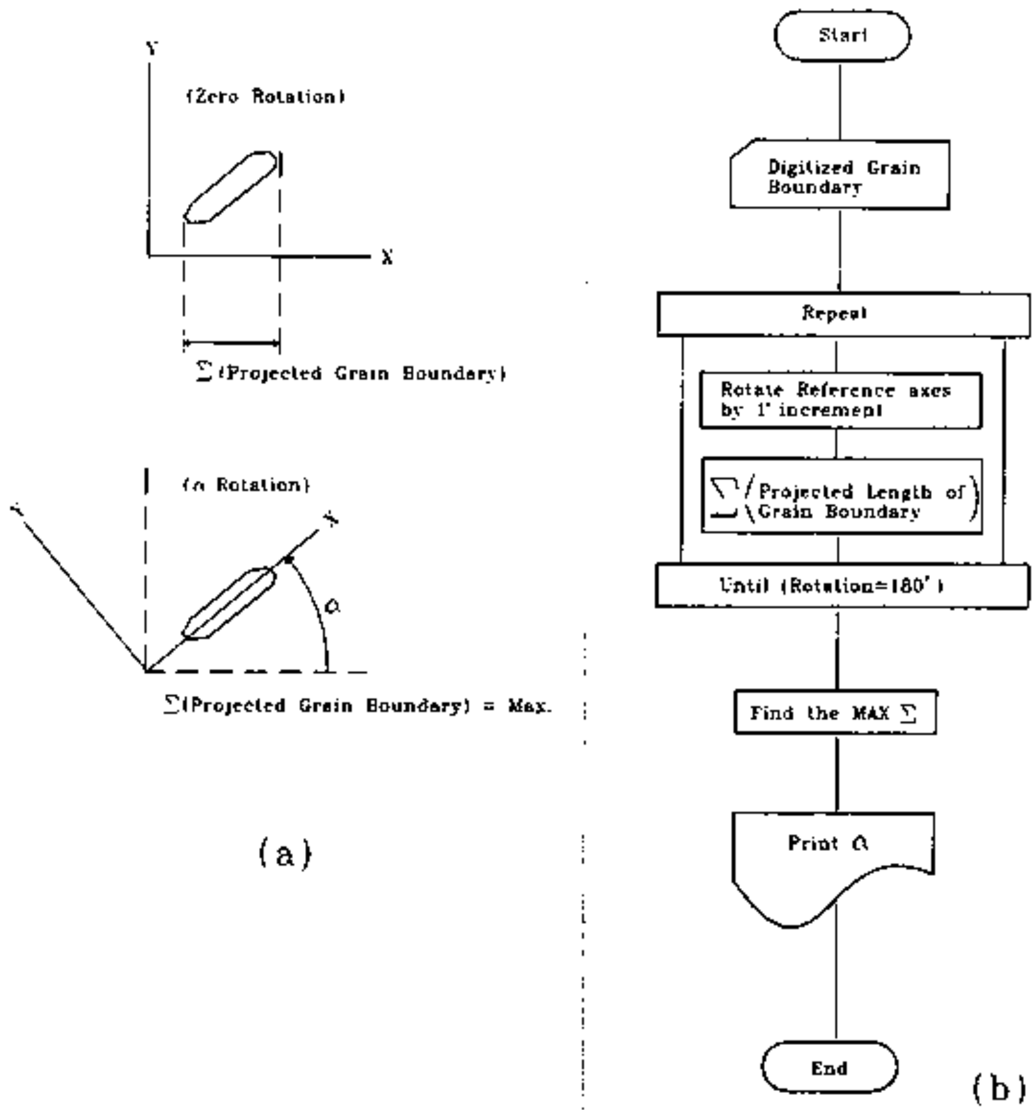

Figure II-6. Principles and the flow chart of the program "GBO" - grain boundary orientation. (a) The sum of the projected grain boundary to the x-axis is calculated after rotation of references axes. After a rotation, the projected length will be the maximum because x-axis is parallel to the grain shape. (b) Flow chart of the program "GBO". The input data for this program is digitized line segments of grain boundary.

III. LITHOLOGY

III-1. GRANITIC GNEISS

The granitic gneiss is mainly composed of quartz and feldspar with small amounts of biotite, clinopyroxene, amphibole and garnet (Figures III-1). The powder X-ray diffraction pattern was matched with JCPDS by Rigaku software. As plotted on the quartz-feldspar-other mineral ternary diagram (Figure III-1 (d)), the amount of quartz and feldspar exceeds 60 percent of the whole rock composition. The color of this rock type, however, is dark, probably due to the grain size reduction and the weathering of oxide and mafic minerals such as ilmenite, amphibole and pyroxene.

On the handspecimen scale the rock has a foliation defined by alternating mafic and felsic layering. On the microscopic scale, the granitic gneiss shows the very distinctive granulite texture of quartzofeldspathic rocks (Nockolds and others, 1978) with long quartz ribbons and aggregates of finely granular quartz and feldspar (Figures III-2 and III-3). Quartz ribbons have subgrain boundaries and cracks generally perpendicular to the long dimension of the ribbon. The grain boundaries in the aggregates are straight or slightly curved, and usually meet at 120° triple junctions. The length of quartz ribbon ranges from a millimeter to 2 centimeters and the average size of individual quartz and feldspar grains in the aggregates is around 0.5 millimeter (Figure III-2).

Accessory minerals include apatite, sphene, rutile and zircon. Weathered products such as sericite and stains associated with amphibole and biotite are also common.

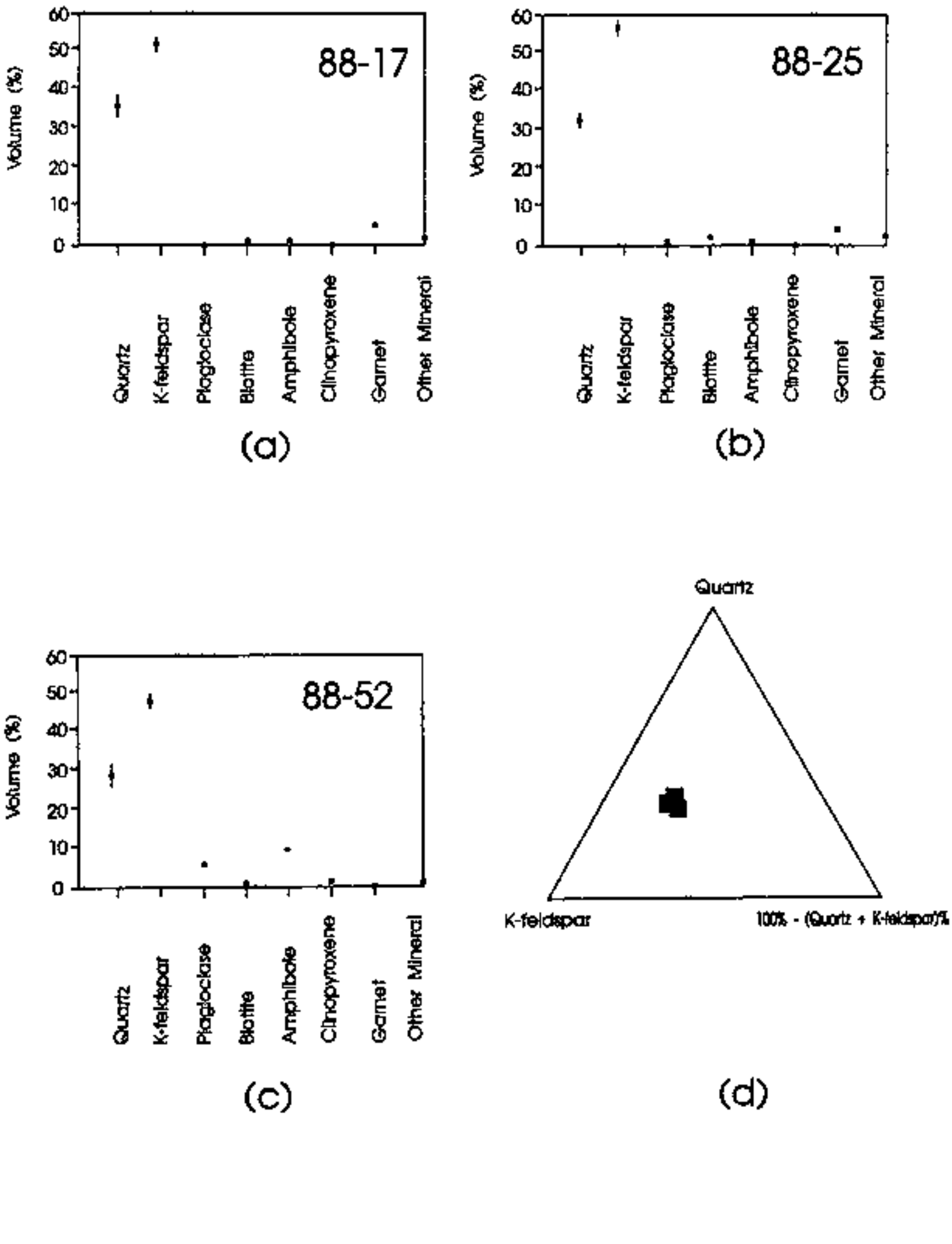
88-17
Volume (%)
0
10
20
30
40
50
60
Quartz
K-feldspar
Plagioclase
Biotite
Amphibole
Clinopyroxene
Garnet
Other Mineral
88-25
Volume (%)
Quartz
K-feldspar
Plagioclase
Biotite
Amphibole
Clinopyroxene
Garnet
Other Mineral
88-52
Volume (%)
Quartz
K-feldspar
Plagioclase
Biotite
Amphibole
Clinopyroxene
Garnet
Other Mineral
Quartz
K-feldspar
100% - (Quartz + K-feldspar)%

(a) (b) (c) (d)

Target:	Cu
Voltage:	45KV
Current:	30mA
Scan Speed:	10°/min.
Step:	0.02°

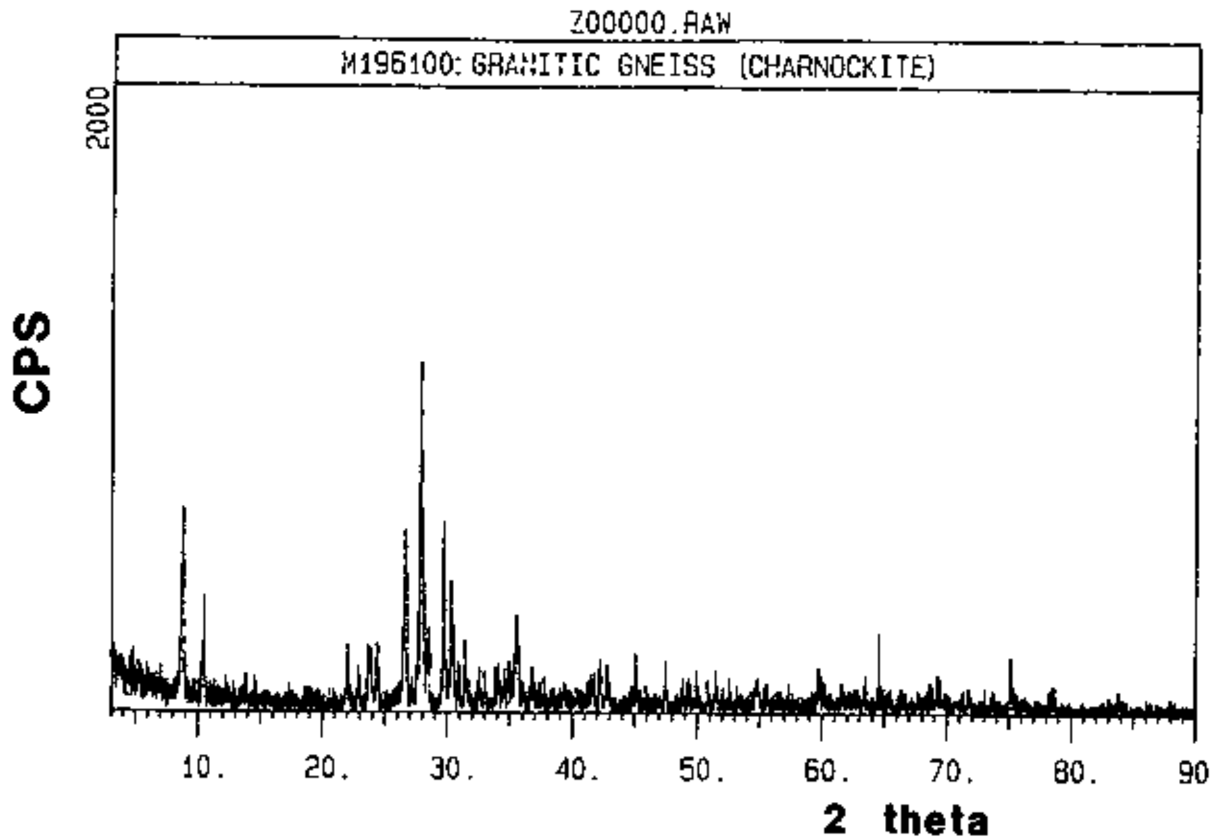

(e)

Figure III-1. Modal mineralogy and powder X-ray diffraction pattern of the granitic gneiss. (a), (b) and (c): Modal mineralogy determined from point counting. "Other Mineral" includes apatite, opaque minerals, and zircon. The error bar is constructed after the method of van der Plas and Tobi (1965). (d) Composition plot on the quartz-potassium feldspar-the rest of minerals ternary diagram. (e) Powder X-ray diffraction pattern from the granitic gneiss.

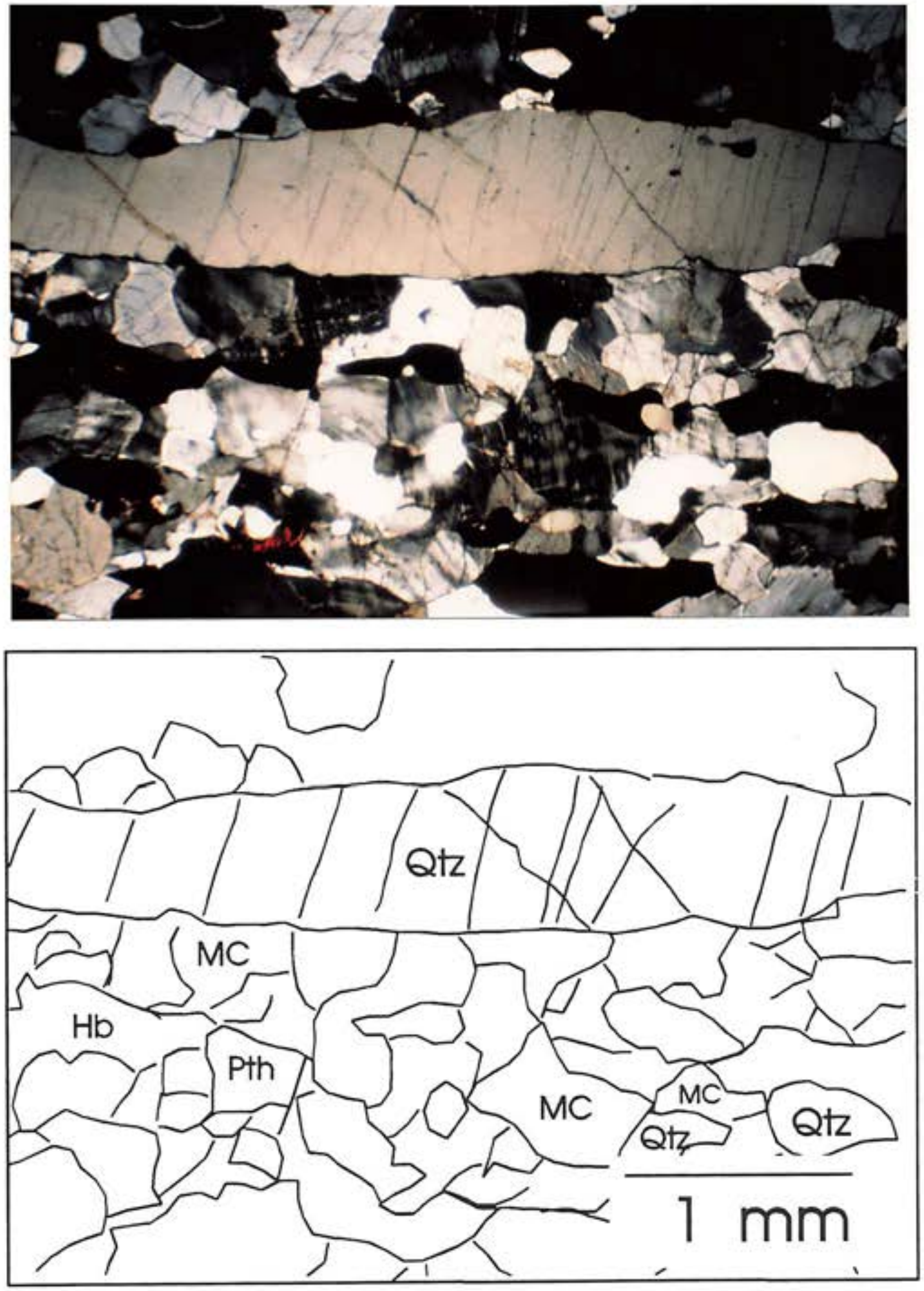

Figure III-2. Crossed polarized light photomicrograph of quartz ribbon in the granitic gneiss. Quartz ribbon and aggregates of finely-granular quartz and feldspar (usually perthite) are present. In the aggregates, the grain boundaries are straight or slightly curved. (Qtz = quartz, MC = microcline, Hb = hornblende, and Pth = perthite)

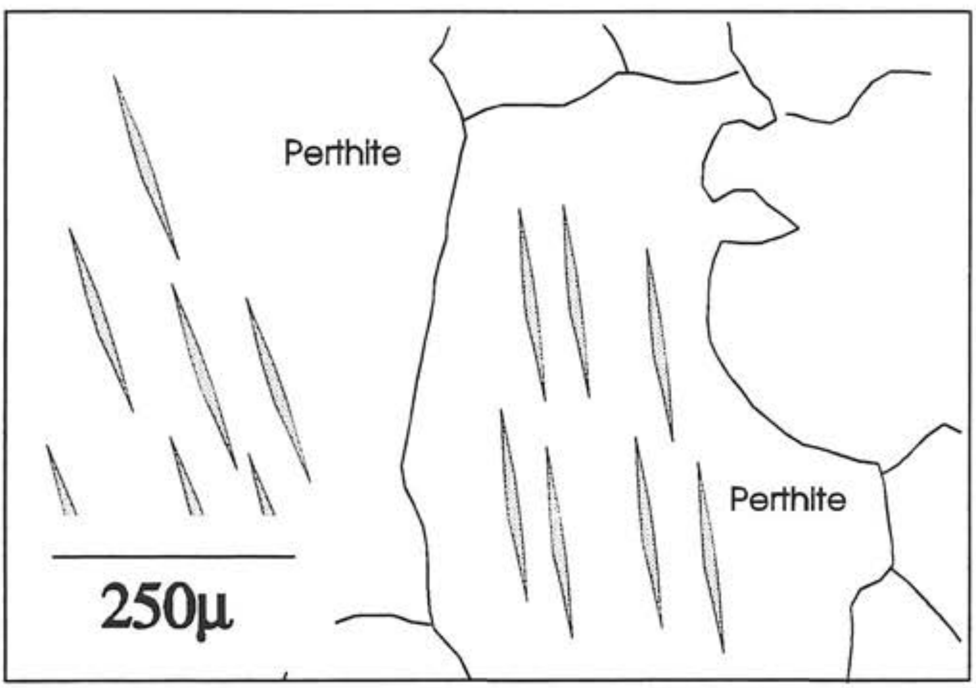

Figure III-3. Crossed polarized light photomicrograph of perthite from the granitic gneiss.

The granitic rock in this study is called charnockite on the New York State Geologic Map (Isachsen and Fisher, 1970). The term charnockite, *sensu stricto*, is the anhydrous granite-mineralogy granulite facies rock which has hypersthene (Nockolds and others, 1978). Hypersthene, however, is not a common mineral in this rock type in the study area. Therefore, a better term to describe this rock is quartzofeldspathic gneiss since it has around 60 to 80 percent quartz and feldspar (Figure III-1 (d)).

III-2. AMPHIBOLITE

The major rock-forming minerals in the amphibolite are plagioclase, amphibole, orthopyroxene, clinopyroxene, biotite, garnet and ilmenite (Figures III-4). Sphene and zircon are present as minor minerals. The overall grain size (0.5 millimeter to 3 millimeter) is larger than that of the granitic gneiss.

Twinned plagioclase grains are common; some examples of tapering twinning are also found. Plagioclase composition (An25 to An45) was determined by the Michel-Levy method.

The common amphibole in this rock is hornblende with ilmenite inclusions. Although there are hornblende-rimming-orthopyroxene contacts (Figure III-5), it is hard to generalize that the hornblende-orthopyroxene contacts are coronatic. Garnets are usually rimmed by plagioclase, and the minerals in contact with this rimming plagioclase are orthopyroxene and amphibole (Figure III-6). These textures are discussed in the metamorphism section at the end of this chapter.

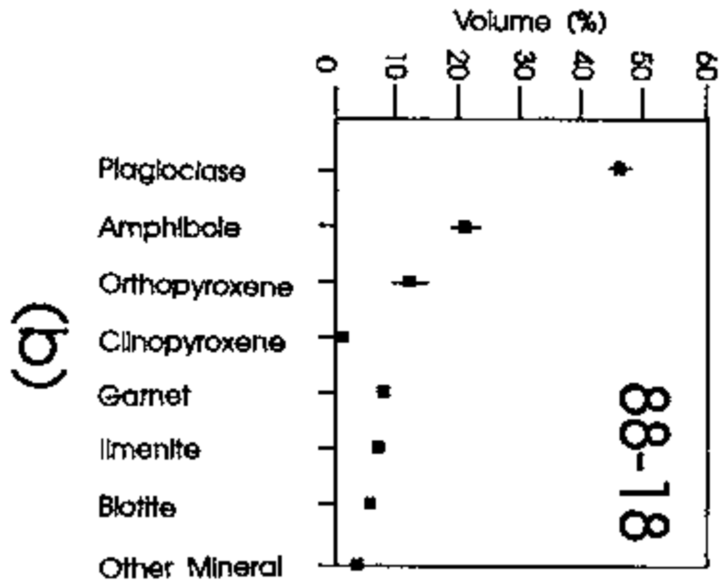
Volume (%)
0
10
20
30
40
50
60
Plagioclase
Amphibole
Orthopyroxene
Clinopyroxene
Garnet
Ilmenite
Biotite
Other Mineral
88-18
(b)

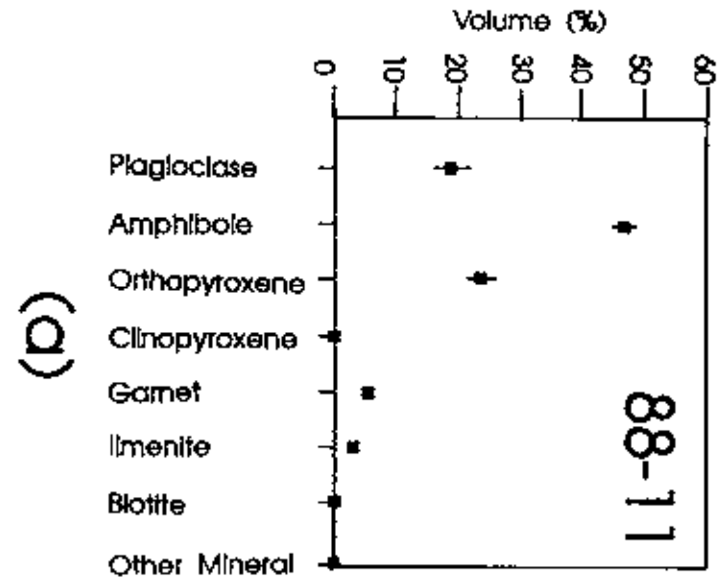
Volume (%)
0
10
20
30
40
50
60
Plagioclase
Amphibole
Orthopyroxene
Clinopyroxene
Garnet
Ilmenite
Biotite
Other Mineral
88-11
(a)

Target:	Cu
Voltage:	45KV
Current:	30mA
Scan Speed:	10°/min.
Step:	0.02°

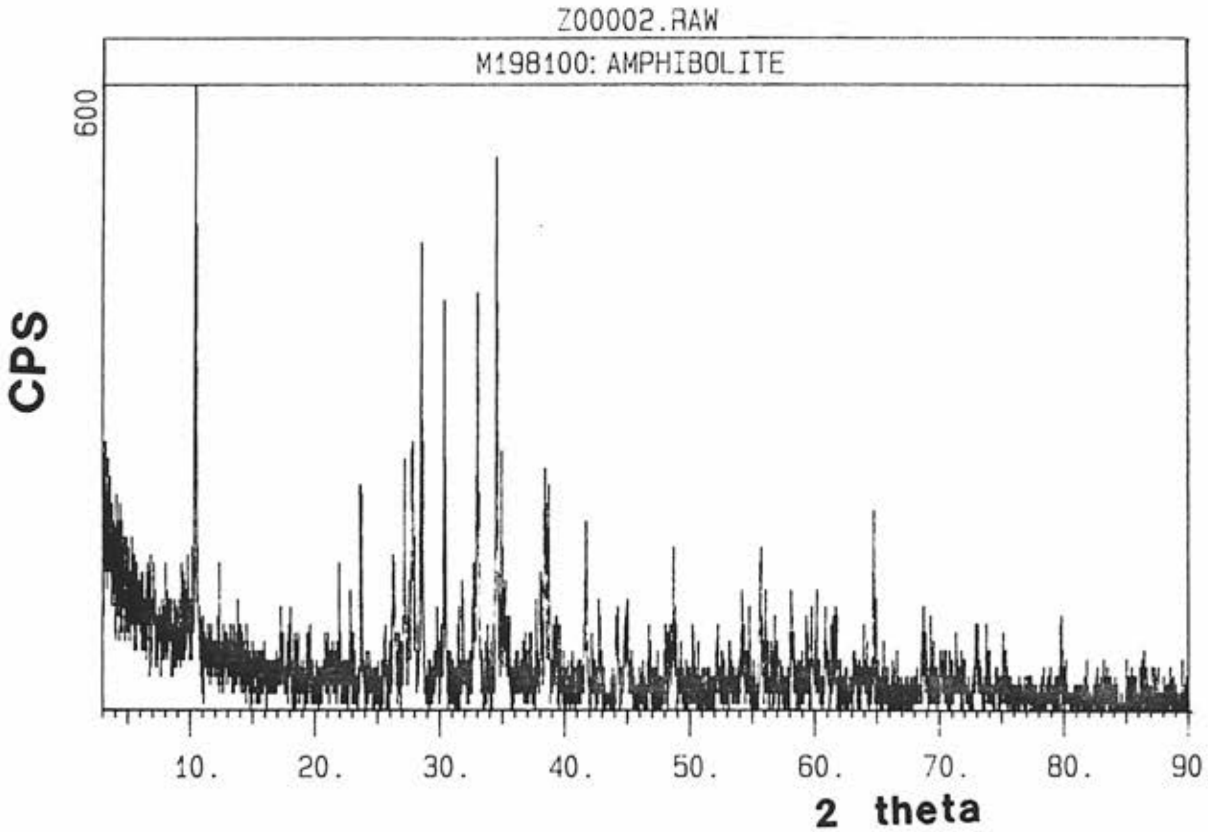

(c)

Figure III-4. Modal mineralogy and powder X-ray diffraction pattern of the amphibolite. (a) and (b): Modal mineralogy determined from point counting. (c) Powder X-ray diffraction pattern.

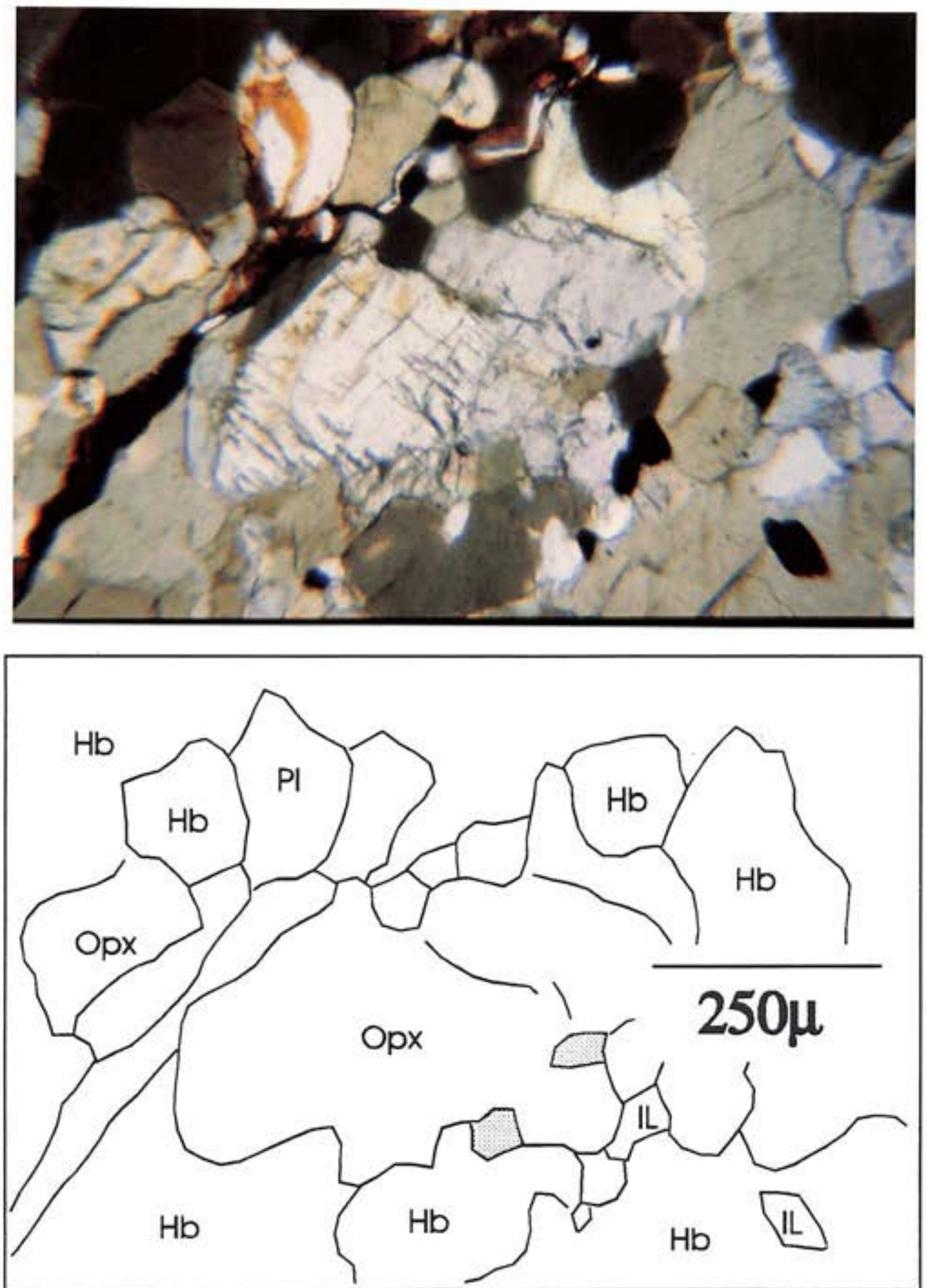

Figure III-5. Plane polarized light photomicrograph of hornblende-orthopyroxene contact in the amphibolite. The dotted grains in the sketch may be secondary (retrograde) hornblende. (Hb = hornblende, Opx = orthopyroxene, IL = ilmenite, and Pl = plagioclase).

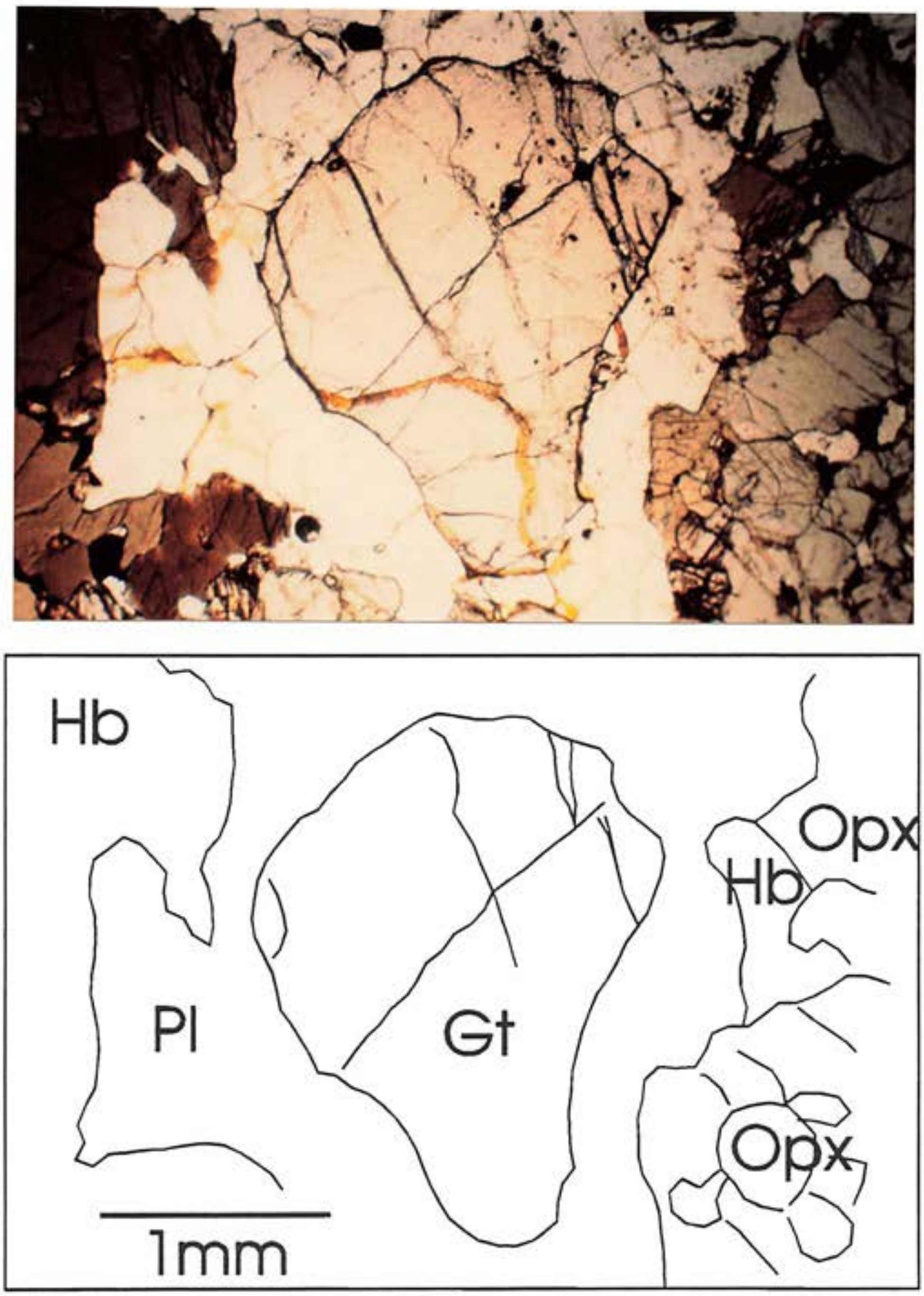

Figure III-6. Plane polarized light photomicrograph of plagioclase-mantling-garnet texture from the amphibolite. (Gt = garnet, Pl = plagioclase, Hb = hornblende, and Opx = orthopyroxene).

III-3. MARBLE

Marble is found in the northwestern part of the field area and is composed of calcite, quartz, orthopyroxene, scapolite, plagioclase and sphene (Figures III-7). Calcite (around 70 volume percent) surrounds other minerals. Calcite shows deformation twins and serrate grain boundaries.

III-4. METAMORPHISM

In the granitic gneiss, perthite, formed by unmixing of plagioclase and K-feldspar, is the most common feldspar. In igneous rock, perthite is very common if the cooling rate (after crystallization) is slow enough so that Na^+ and K^+ ions can diffuse and migrate. The perthites in this granitic gneiss, however, may possibly have a metamorphic origin, i.e., without melting. This is possible because the temperature of granulite facies is high enough to reach the spinoidal curve.

The overall grain size in the amphibolite is larger than that of the granitic gneiss. This is thought to be due to the rheological difference between the easily deformed quartz-rich mineralogy and the more competent plagioclase-amphibole-orthopyroxene mineralogy during the ductile deformation. More sodic plagioclase (An25 to An45) may also imply the effect of hydrous shear zone deformation because calcium depletion in plagioclase is a common phenomenon during hydrous shear zone deformation (Beach, 1980).

Some of the orthopyroxene-hornblende contacts in the amphibolite (Figure III-5) which consist of hornblende rimming orthopyroxene suggest the formation of hornblende (dotted grains in Figure III-5) by hydrous retrograde metamorphism.

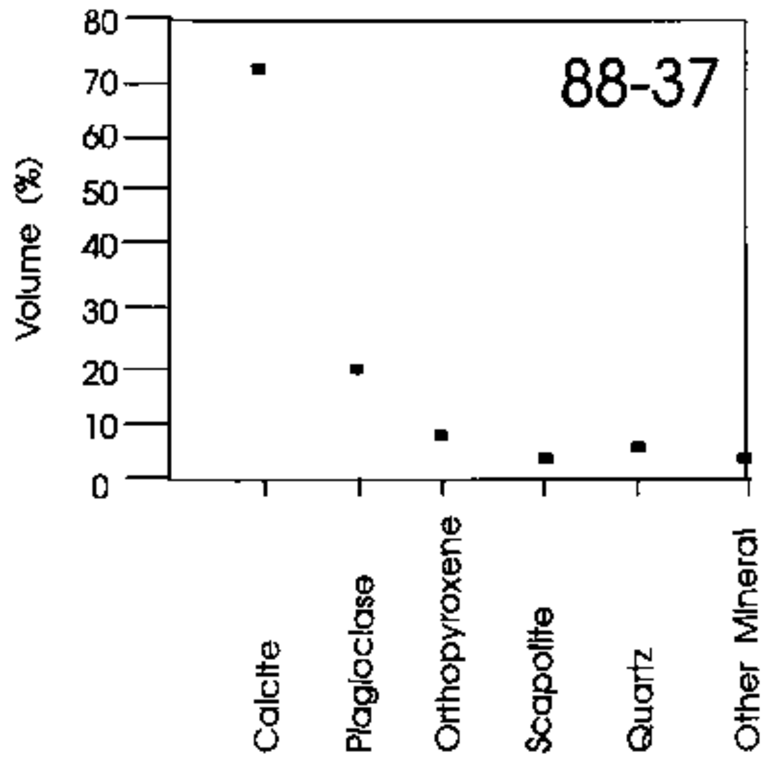

88-37
Volume (%)
0
10
20
30
40
50
60
70
80
Calcite
Plagioclase
Orthopyroxene
Scapolite
Quartz
Other Mineral

(a)

Target: Cu
Voltage: 45KV
Current: 30mA
Scan Speed: 10°/min.
Step: 0.02°

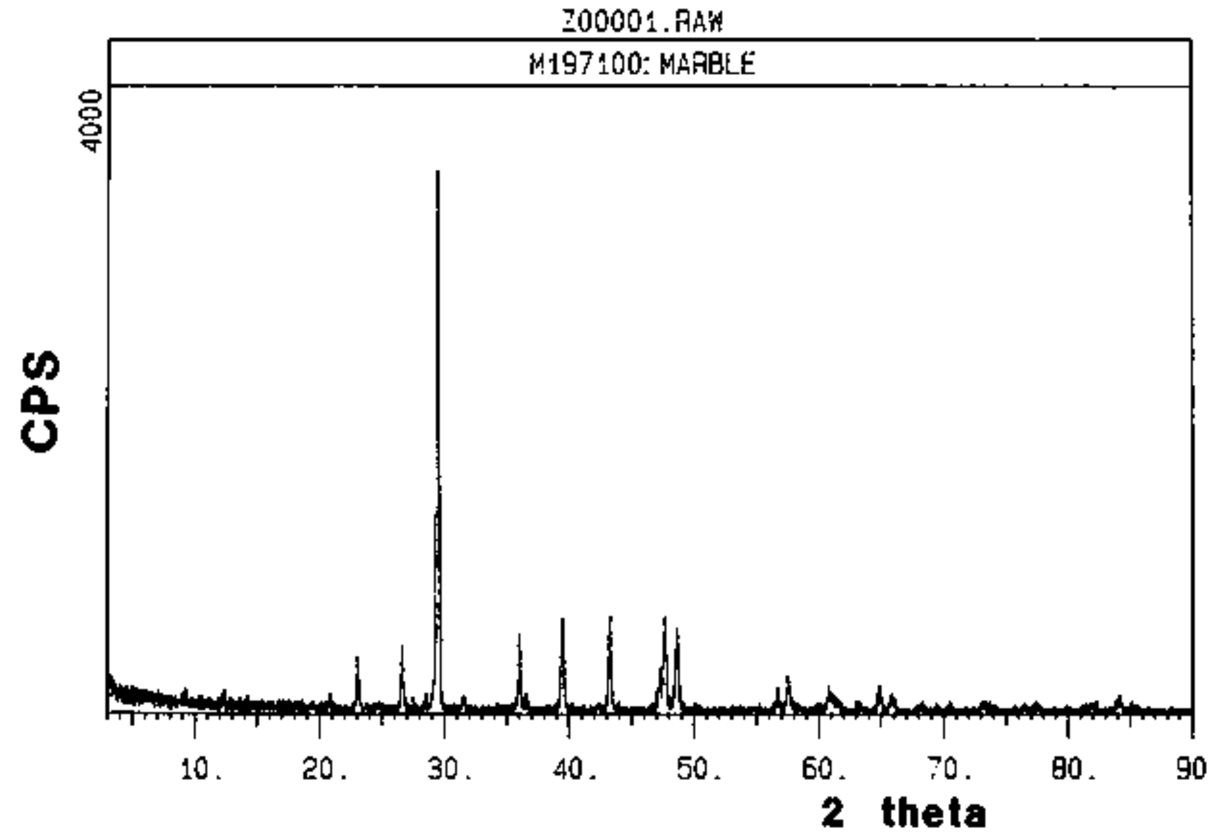

(b)

Figure III-7. Modal mineralogy and powder X-ray diffraction pattern of the marble. (a) modal mineralogy determined from point counting. (b) Powder X-ray diffraction pattern.

One of the following chemical reactions may explain the formation of secondary hornblende by the hydrous retrograde metamorphism;

{ Hypersthene + Clinopyroxene + Plagioclase + H_2O }

→ { Hornblende + Quartz }

or

{ Hypersthene + Plagioclase + H_2O }

→ { Hornblende + Almandine + Quartz }

-Reactions from Winkler (1979, p. 265)

For most of the hornblende, however, it is hard to interpret the formation of hornblende by the above retrograde reactions since first, the above reactions form quartz as a product which is not common in the amphibolite, and second, the straight hornblende grain boundaries is more adequately interpreted as primary rather than secondary. Another way of interpreting the coexistence between orthopyroxene and hornblende is in terms of P_{water} (water pressure) during metamorphism. According to De Waard's subfacies model (1965) of the granulite facies, the granulite facies can be divided into six subfacies in P_{load} and P_{water} space. In his subfacies model, hornblende occurs as P_{water} increases (e.g. from orthopyroxene-plagioclase subfacies to hornblende-orthopyroxene-plagioclase subfacies). The hornblende in the amphibolite, therefore, can be interpreted as primary hornblende formed during high P_{water} granulite facies metamorphism.

Plagioclase-mantling-garnet texture (Figure III-6) can be explained by the effect of a pressure decrease during metamorphism. Garnet is a denser repository for Ca and Al than anorthite at high pressure so garnet decomposes to anorthite with a pressure decrease. In pelitic rocks, the following reaction as a result of decompression has been documented:

{ Garnet + Sillimanite }

$\rightarrow$ { Plagioclase } (with pressure drop)

-Reaction from Lonker (1980)

The age of granulite facies metamorphism is 1150 to 1000 Ma (Bohlen and Mezger, 1989), and the estimated temperature and pressure range for granulite facies metamorphism is 750 to 825 °C and 0.70 to 0.85 GPa, respectively (Bohlen and Mezger, 1989).

IV. STRUCTURAL GEOLOGY

IV-1. INTRODUCTION

A shear zone is defined as "*a zone with subparallel walls in which high deformations are localized. Such zones can show strain discontinuities across a plane (a fault), or the strain variation may be continuous across the zone such that, on the scale of a rock outcrop, no geometrical discontinuities can be seen (a ductile shear zone).*" (Ramsay and Huber, 1983, p. 53). In other words, a brittle shear zone has a discontinuity (fault) which divides the almost undeformed walls of the shear zone while tracing the layers is possible in a ductile shear zone because there is no discontinuity. Ductile shear zones are extremely common in deformed crystalline basement rocks (granites, gabbros, gneisses) which have been deformed under metamorphic conditions of greenschist, blueschist, amphibolite and granulite facies (Ramsay, 1980).

Mylonite, originally, was the term to describe a rock formed by apparently brittle deformation which shows such textures as "crushed", "dragged" or "ground out". However, it is possible to have an almost identical-looking rock by ductile deformation with recovery and recrystallization. Bell and Etheridge (1973) proposed a new definition of mylonite: "*A mylonite is a foliated rock, commonly lineated and containing megacrysts, which occurs in narrow, planar zones of intense deformation. It is often finer grained than the surrounding rocks, into which it grades.*" According to Bell and Etheridge's definition, there is room for the ductile-deformation mylonite. The usage of "mylonite" in this study will refer to the mylonite which has a ductile deformation origin.

In Ramsay's (1980) definition of shear zone, the words "*narrow*" and "*localization of deformation*" are used. It is worthwhile to think about why these terms are used. In the low temperature mechanical tests of rocks, stress must be increased for a strain increase because the movement of dislocations is limited by obstacles (strain hardening) (Figure IV-1). This stress increase is not quite realistic in geology. However, in high temperature deformation of rocks, stress increase is not necessary due to strain softening processes such as recovery and recrystallization. Therefore, the narrow shear zone (localized zone of deformation) is possible due to strain softening processes. Without strain softening (recovery in the broad sense), all of the rocks of the crust would be deformed up to the degree of strain hardening. Genetically, a shear zone can be defined as a zone of strain softening (White and others, 1980).

During petrographic work, microstructures indicating plastic deformation of minerals were observed; the shear zone model was based on these. The following sections describe the macroscopic and microscopic structures and interpret these structures to test the shear zone model.

IV-2. MACROSCOPIC STRUCTURES

Observation

The foliations in this area are subhorizontal and very consistent throughout the field area (Figure IV-2). In the granitic gneiss, they are defined by alternating mafic and felsic layers. Mafic layers are composed of amphibole, pyroxene, biotite, garnet, and ilmenite. Felsic layers are usually made up of quartz and

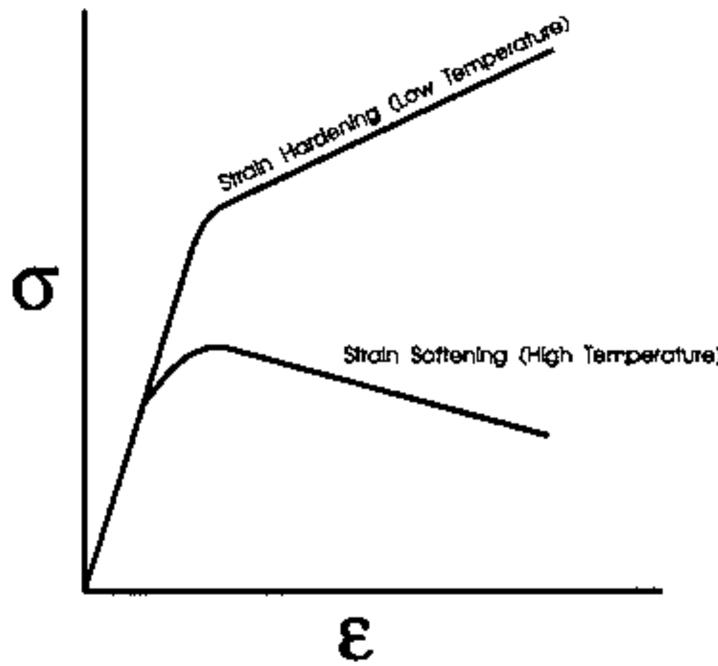

Figure IV-1. Stress and strain curve, illustrating the strain hardening and strain softening.

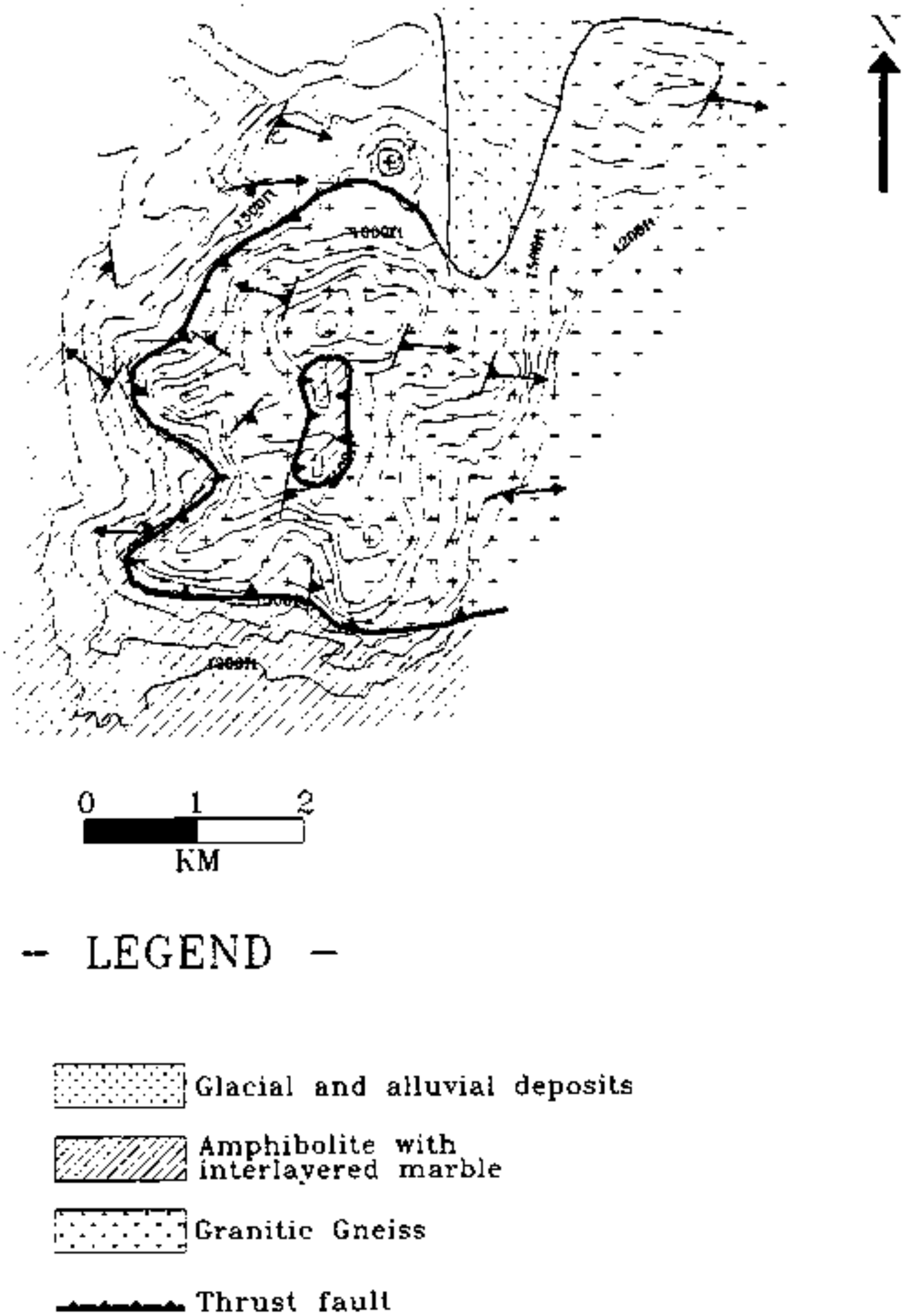

Figure IV-2. Structural map of the study area and equal area projection of foliations and lineations on the stereonet. The lithologic boundary in the southern part is drawn after the New York State Geologic Map (Isachsen and Fisher, 1970).

feldspar. The thickness of each layer ranges from 2 millimeters to 5 centimeters. In the amphibolite, foliations are weaker than in the granitic gneiss.

The lineations are east-west trending and their plunging angle is also fairly consistent throughout the area (Figure IV-2). Lineations are defined by the long dimensions of minerals such as quartz and amphibole. Quartz lineations can be easily detected by touching the foliation surface because quartz is more resistant to weathering than other minerals present.

There are two major contacts between the amphibolite and the granitic gneiss, one around the 1600 ft. contour line and the other around the 2000 ft. contour line (Figure IV-2). At the contact, highly strained granitic gneisses and folded amphibolites are present (Figure IV-3).

Interpretation

Strong subhorizontal foliations and east-west trending lineations together with microstructures (discussed below) provide the evidence for the shear zone deformation in this area. Lineation is assumed to be the direction of motion since finite stretching direction becomes parallel to the stretching lineation for large amounts of strain.

Around the lithologic contact, highly strained granitic gneiss and folded amphibolite are observed (Figure IV-3). These structures are interpreted to be related to the rheological difference between the granitic gneiss and the amphibolite. The difference in flow behaviors of these two rocks seems to be related to the compositional difference.

Figure IV-3. Lithologic contact between the granitic gneiss (at the top) and the amphibolite (at the bottom). The lithologic contact is at the hammer head. The station number for this outcrop is 89-6 (see Figure I-2).

Although the most highly strained rocks are found at the lithologic contact, the whole area (in a vertical sense) seems to be highly deformed, since both planar and linear fabric with plastic deformation microstructures is found consistently across the whole area. Therefore, a large scale (km. scale) ductile shear zone is suggested.

IV-3. MICROSCOPIC STRUCTURES: OBSERVATION

Feldspar

Perthites are the most common feldspar in the granitic gneiss and found in aggregates with quartz. The grain boundaries between perthite-perthite and perthite-quartz are straight or slightly curved (Figure III-2). The average grain size is about 0.5 millimeter and unimodal (no megacrysts). The correlation of microcline twins and plagioclase lamellae between neighboring perthites is poor. Some plagioclase in the amphibolite shows tapering twinning and subgrain boundaries (Figure IV-4).

Quartz

In the granitic gneiss quartz is present as either ribbons or aggregates with perthite (Figure III-2). The length of quartz ribbons ranges from 1 millimeter to 2 centimeters. The quartz ribbons are usually made up of multiple small grains with both low and high angle boundaries. Subgrain boundaries (deformation bands) are very common and their orientation is generally perpendicular to the long dimension

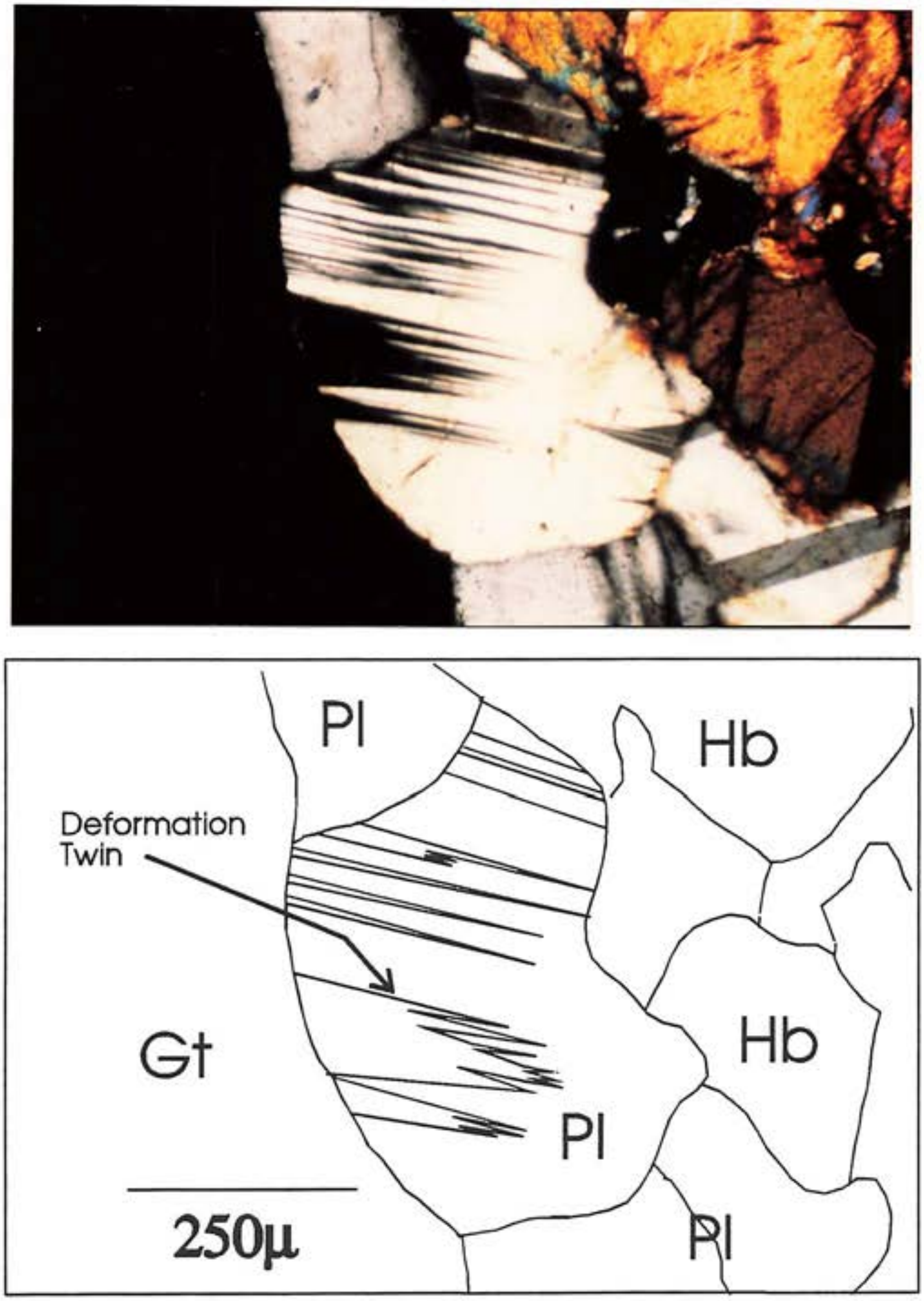

(a)

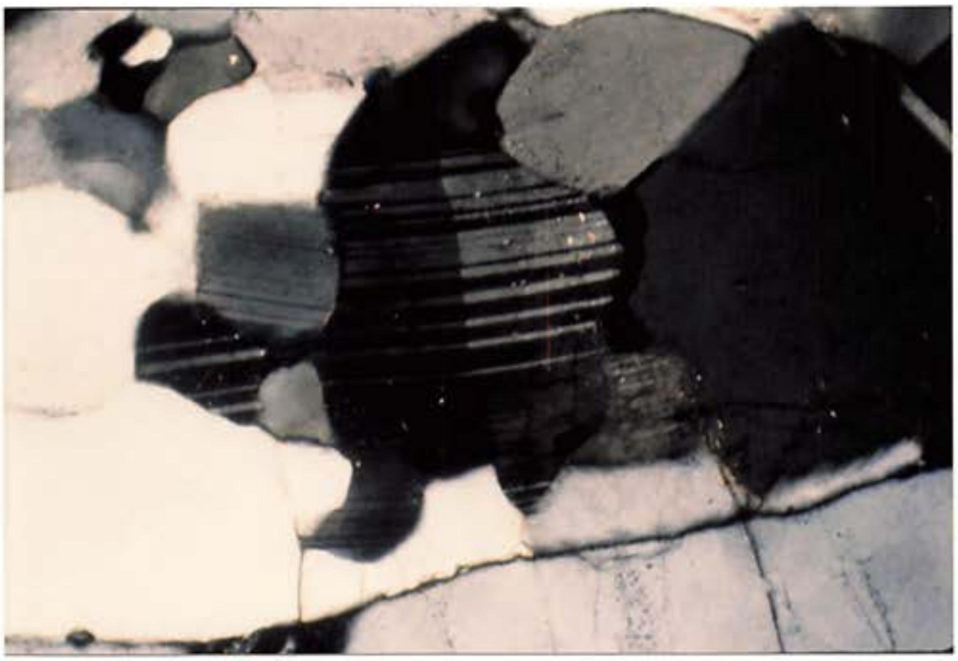

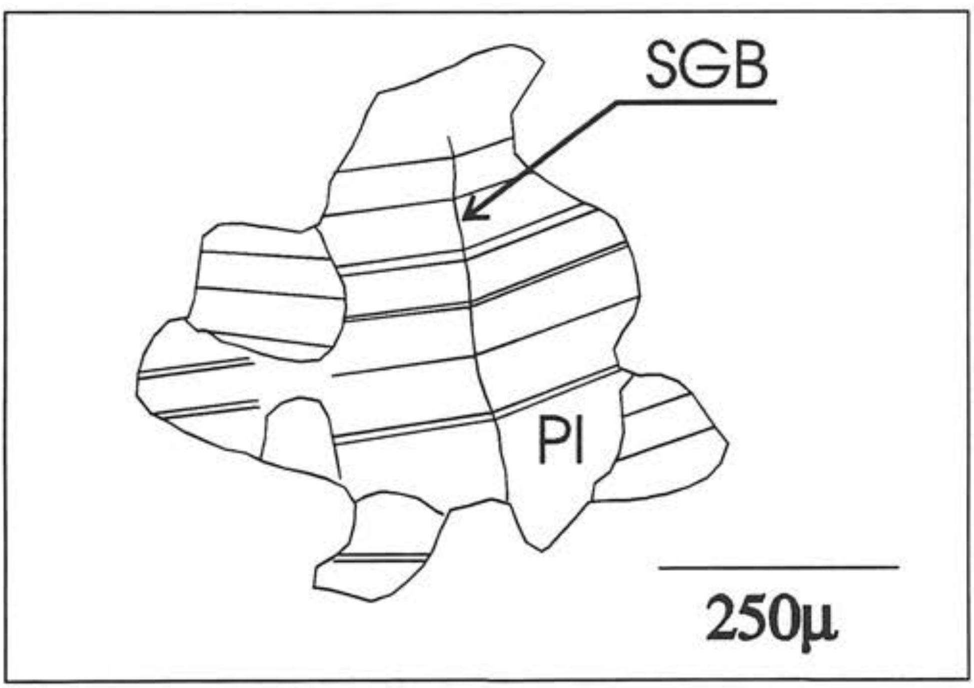

(b)

Figure IV-4. Crossed polarized light photomicrograph of plagioclase deformation microstructures; (a) Deformation twin, (b) Subgrain boundary. (Pl = plagioclase, Hb = hornblende, and Gt = garnet) of the ribbon. The overall c-axis pattern in quartz ribbons is perpendicular to both foliation and lineation. Pinning is also found in the quartz ribbons (Figure IV-5). Most of the quartz ribbons show cracks perpendicular to the long dimensions of the ribbon.

In aggregates, the average grain size of quartz is almost the same as that of perthite (0.5 millimeter). The c-axis pattern from the aggregates is not so concentrated as the pattern from the ribbon.

Calcite

The most dominant microstructure of calcite is twinning (Figure IV-6). The grain boundaries between adjacent calcite grains are serrate (Figure IV-6).

Biotite and amphibole

Grains of biotite in the mafic layer have preferred crystallographic orientation. The (001) cleavage plane of biotite is aligned parallel to the foliation defined by compositional layering. The long dimensions of amphibole grains are aligned parallel to the lineation.

IV-4. MICROSCOPIC STRUCTURES: INTERPRETATION

Feldspar

Experimental studies (Tullis and Yund, 1985; Tullis and Yund, 1987) of K-feldspar show that there are two major deformation regimes in feldspar: 1)

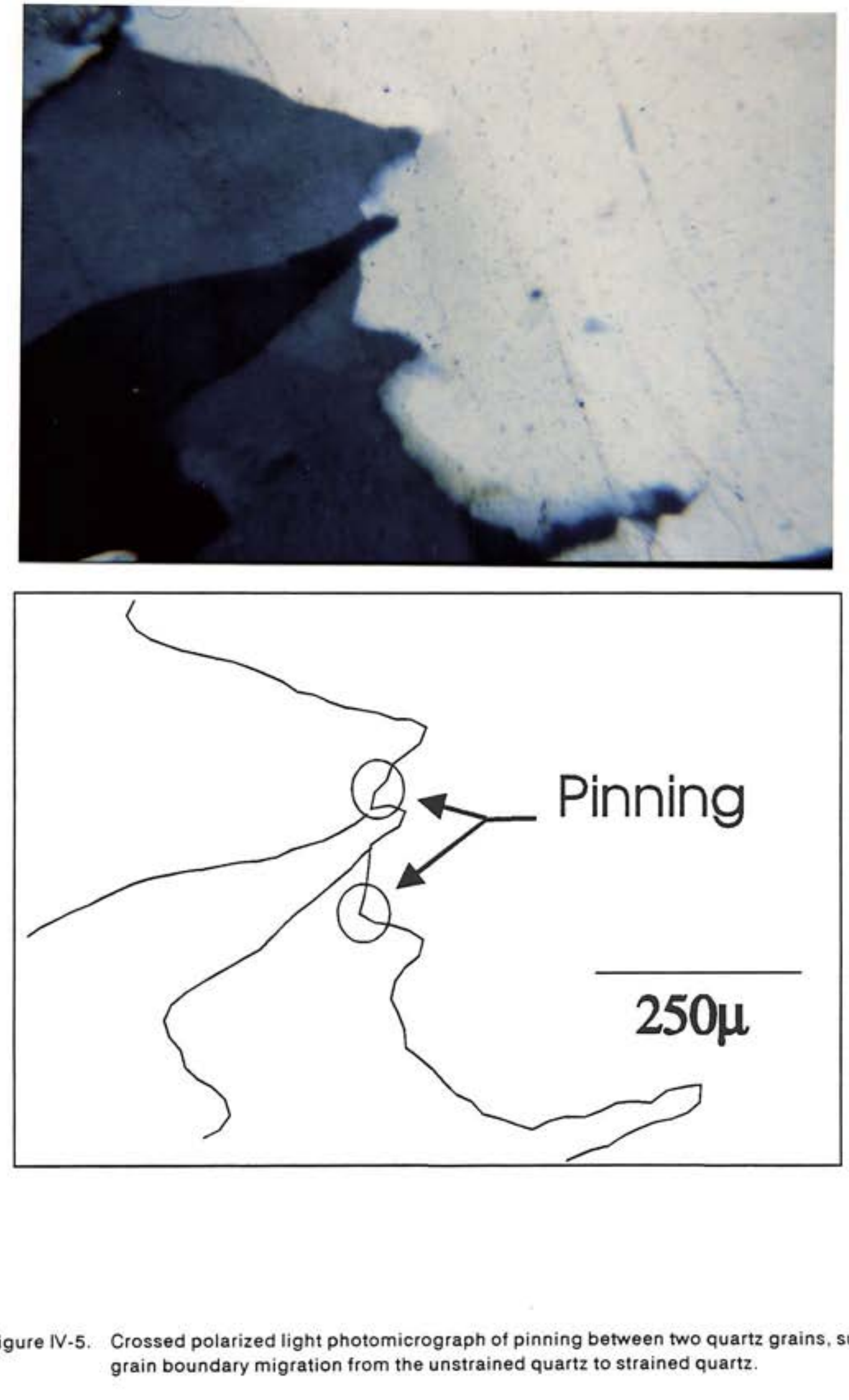

Figure IV-5. Crossed polarized light photomicrograph of pinning between two quartz grains, suggesting the grain boundary migration from the unstrained quartz to strained quartz.

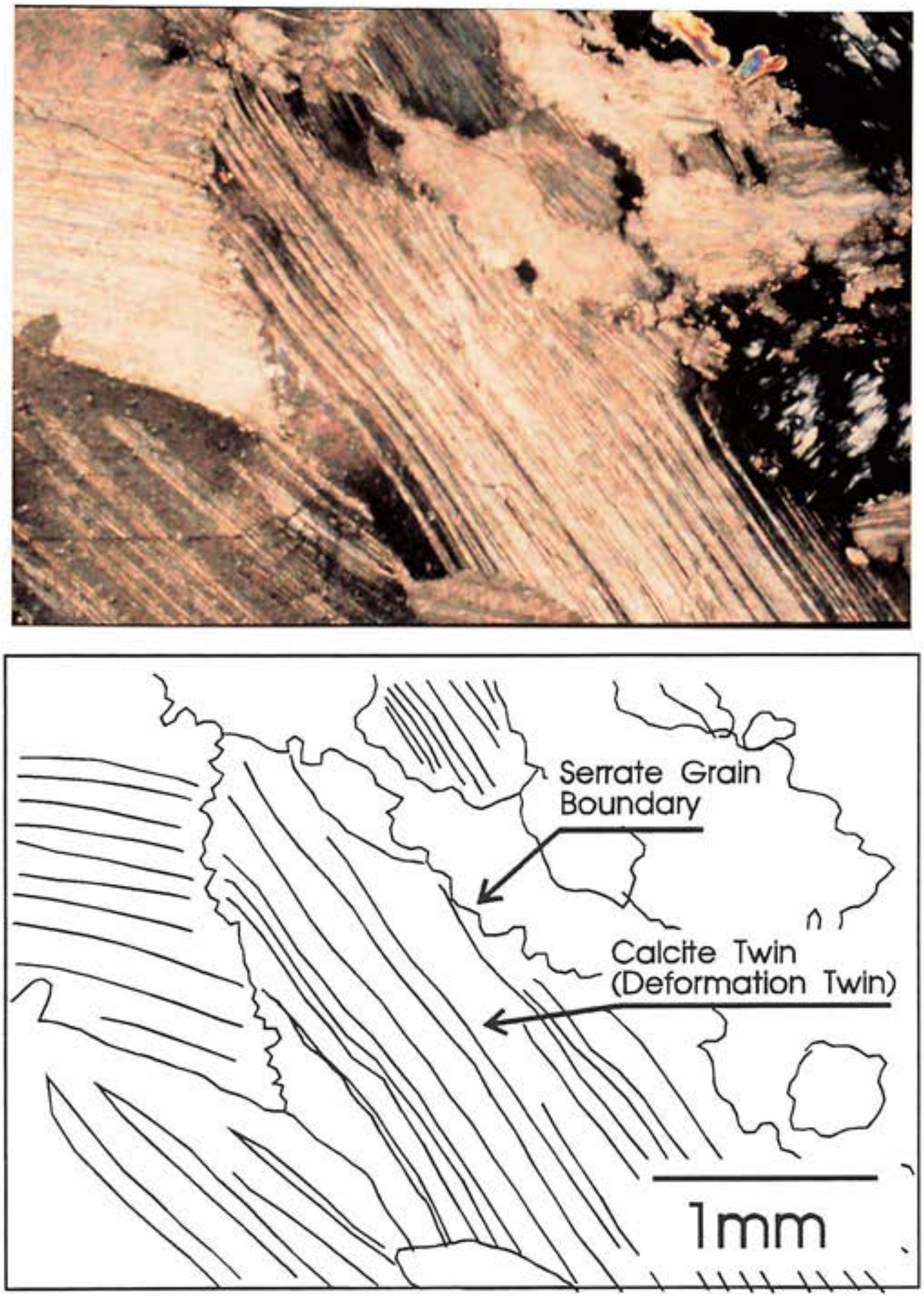

Figure IV-6. Crossed polarized light photomicrograph of deformed calcite from the marble.

dislocation creep and 2) cataclastic flow. In dislocation creep (temperature equivalent to upper amphibolite and granulite facies metamorphism), the major strain softening mechanism is dynamic recrystallization (Tullis and Yund, 1985). A common microstructure produced by dynamic recrystallization in dislocation creep is mantle-core texture. The feldspar cores are fairly undeformed and large whereas the mantle is made up of small grains formed by dynamic recrystallization of rim-feldspar. Therefore the grain size distribution will be bimodal since there are large megacrysts (core) and small new grains (mantle). The small new recrystallized grains will share common features (crystallographic orientation and composition) between the neighboring grains.

In the cataclastic flow regime (up to lower amphibolite facies metamorphism), the dominant microstructure is grain size faulting (Tullis and Yund, 1987). Grain size faulting is a small scale (grain scale) inter- and intra-grain faulting. The analogy for this deformation is sugar and/or salt grains in the bottle flowing through a narrow bottle neck (Figure IV-7 (a)). Therefore, the composition and the crystallographic orientation do not have to match between neighboring grains.

The perthites from the granitic gneiss have unimodal grain size distribution and almost no common features with neighboring grains. Therefore it is likely that the microstructures coincide with the cataclastic flow regime. However the following processes can produce the same microstructures: (1) complete dynamic recrystallization at dislocation creep (no megacryst left) with slight rotation of new grains (Figure IV-7 (b)) (it will make comparison between neighboring perthites difficult on a microscope if the starting plagioclase lamellae shape is irregular), or (2) cataclastic flow after complete dynamic recrystallization(Figure IV-7 (c)). To

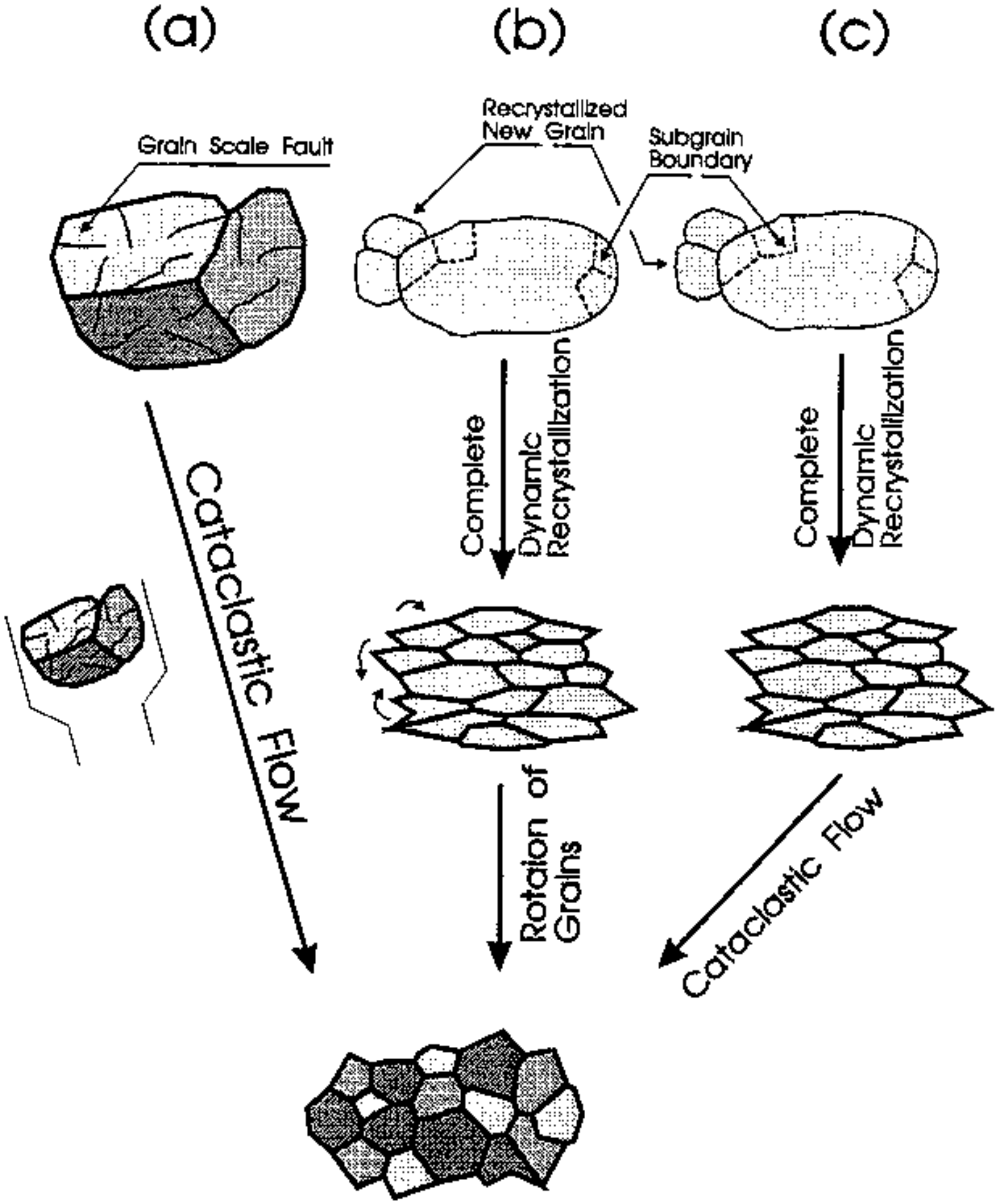

Figure IV-7. Feldspar deformation mechanism. (a) Cataclastic flow. (b) Slight rotation of grains after the complete recrystallization. (c) Cataclastic flow after the complete recrystallization be sure about the feldspar deformation regime, one needs to compare the geochemistry between neighboring feldspar grains and this work was not done in this study.

Plagioclase in amphibolite shows tapering twins which is a common deformation microstructure in the temperature conditions of amphibolite and granulite facies metamorphism (Ji and Mainprice, 1990).

Quartz

Subgrain boundaries are common features of quartz ribbons; the mechanism for formation of subgrain boundaries and the reason why the subgrain boundary is nearly parallel to the c-axis are illustrated in Figure IV-8. When torque is exerted on the crystal, the crystal will be bent to cause undulose extinction since the orientation of the c-axis is gradually changing (Figure IV-8 (a) and (b)). If the shape of the bent crystal remains unchanged, dislocations, which are geometrically necessary, will be formed (Figure IV-8 (c)). To lower the strain energy, dislocations will migrate and annihilate each other. If not annihilated, dislocations will be tangled and form subgrain boundaries nearly parallel to the c-axis (Figure IV-8 (d)). Sub-parallelism between subgrain boundaries and the c-axis is possible if the working slip plane is the basal plane.

The regime of dislocation creep for quartz can be divided into two domains: (1) prismatic slip domain (high temperature), (2) basal slip domain (low temperature). The transition between these two domains occurs at the temperature condition of lower amphibolite facies metamorphism. The model of different slip systems for quartz at different temperatures is based on a comparison of regional

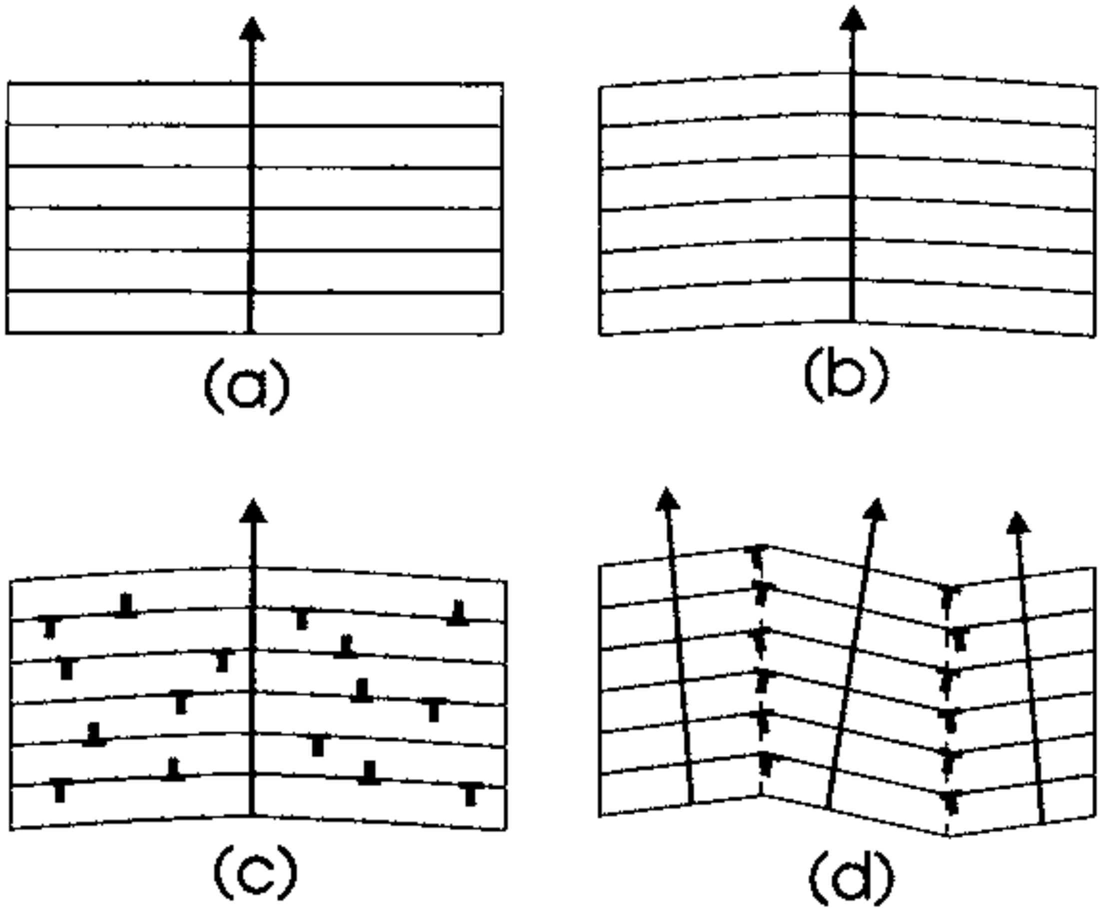

Figure IV-6. Stages of subgrain development in the quartz (Nicolas and Poirier, 1976). (a) undeformed crystal. (b) elastic bending. (c) formation of geometrically necessary dislocations. (d) formation of subgrain boundaries.

geology (metamorphism) to c-axis pattern (Bell and Etheridge, 1976; Miller and Christie, 1981). In the quartz ribbons, subgrain boundaries perpendicular to the foliation and lineation are most common, which suggests the basal <a> slip. The inferred temperature for the quartz ribbon formation, therefore, is lower than the temperature condition of lower amphibolite facies metamorphism.

Pinning (Figure IV-5) is thought to be formed by grain boundary migration from strain-free quartz to strained quartz. In this process, a grain of higher dislocation density, hence higher free energy, is consumed by the dislocation free grain and dislocations are absorbed at the grain boundary (Poirier, 1985). Mantle-core texture is found in the quartz. These textures, pinning and mantle-core, are related to strain softening processes. Cracks found in the ribbons are interpreted as microstructures related to the later uplift since there is no material in these cracks.

Calcite

Twins and serrate grain boundaries are observed in the marble (Figure IV-6). The temperature of transition between the twinning regime and the grain boundary migration regime is around that of lower greenschist facies metamorphism (Schmid and others, 1987).

IV-5. SHEAR SENSE INDICATORS

To describe the nature of a flow, vorticity, which is defined as the sum of the angular velocity of two orthogonal lines, is used (Passchier, 1987). A special case of flow is pure shear flow when the kinematic vorticity number is zero.

Another special case is simple shear flow when the kinematic vorticity number is one. A general flow whose vorticity number is between zero and one is non-coaxial flow, and simple shear flow is a special case for non-coaxial flow. In a non-coaxial flow, the sense of vorticity which is the orientation of the vorticity vector is loosely known as the sense of shear. When describing the shear sense, terms such as "clockwise" or "counter-clockwise" are used. The danger, when using such a terminology as "clockwise or counter-clockwise", is that the nature of flow (usually the range of kinematic vorticity number is between 0 and 1) can be omitted. For example, it is possible to have almost coaxial flow with clockwise shear sense (when kinematic vorticity number=0.1). Therefore, when dealing with the shear sense, one must not assume the flow as simple shear flow. Shear sense indicators used in this study are quartz c-axis fabric, S- and C- cross cutting relationship and outcrop scale folding. The result from these indicators will be explained.

Shear Sense from quartz c-axis pattern

Figure IV-9 (a) shows the quartz c-axis pattern observed from ribbons. As explained in Chapter II, only low-plunging-angle c-axes are represented on this figure. Figure IV-9 (b) illustrates how the c-axis rotates with simple shearing in two dimensions (Etchecopar, 1977). One thing to note is that the c-axis is rotating in the opposite way to shear sense while the slip plane is rotating with same sense. The shear sense from the c-axis pattern is slightly counter-clockwise dominant, which is equivalent to the hanging wall to the west shear sense (Figure IV-9 (a)).

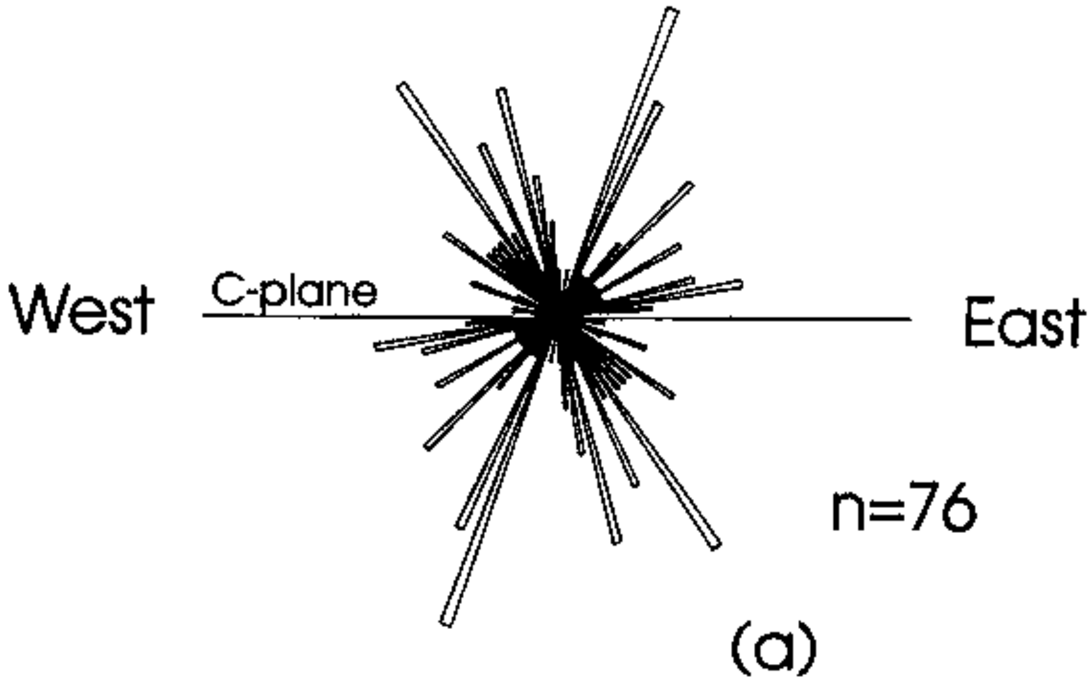

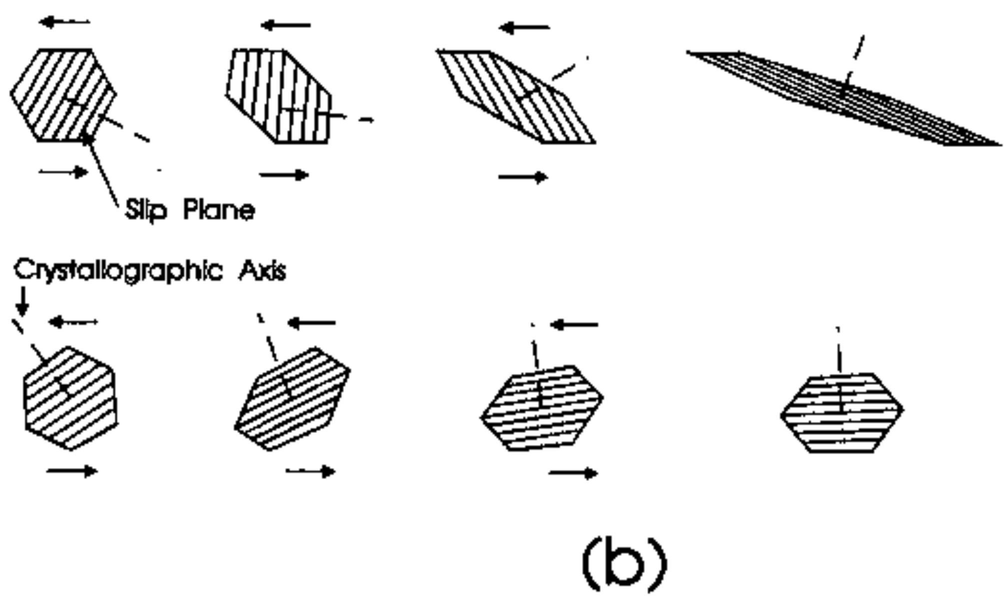

Figure IV-9. c-axis pattern from the quartz ribbon. (a) c-axis pattern on the Rose diagram. (b) rotation of c-axis with simple shearing (Etchecopar, 1974).

Shear Sense from S-C fabric

The term S-C mylonite was first used by Berthe and others (1979) in describing the evolution of mylonitic fabric found in granitic gneiss. They described the S-surface as a surface related to the accumulation of finite strain and the C-surface as a surface of localized high shear strain or a shear zone boundary. Their explanation for the origin of S-C fabric is, "the simultaneous development of the S- and the C- fabric during mylonitization" (p.31, Berthe and others, 1979). Later, Lister and Snoke (1984) regarded this type of mylonite as Type I S-C mylonite and added another category, Type II S-C mylonite. Type II S-C mylonite is usually found in deformed quartz-mica-rich rock whereas Type I S-C mylonite is found in quartz-mica-feldspar rock. Type II S-C mylonite also differs from Type I S-C mylonite in the S-fabric-defining mineral. In Type II S-C mylonite, the S-fabric truncating the C-fabric is defined by quartz grain boundaries, whereas preferred orientation of mica which is asymptotic to the C-fabric is defining the S-fabric in Type I S-C mylonite. However, the determination of sense of shear using the geometry of S- and C- fabric is identical in Type I and II S-C mylonites as shown in Figure IV-10.

Figures IV-11 shows the raw data (traced grain boundaries of mafic and felsic minerals) and result from the program "GBO" (grain boundary orientation) calculation. The maximum grain shape orientation values are found at 3° and 1° relative to horizontal line (short edge of the paper), for mafic minerals and felsic minerals, respectively. There is 2° difference between the orientations of mafic layering and long dimension of felsic minerals, perhaps indicating hanging wall to the west sense of shear.

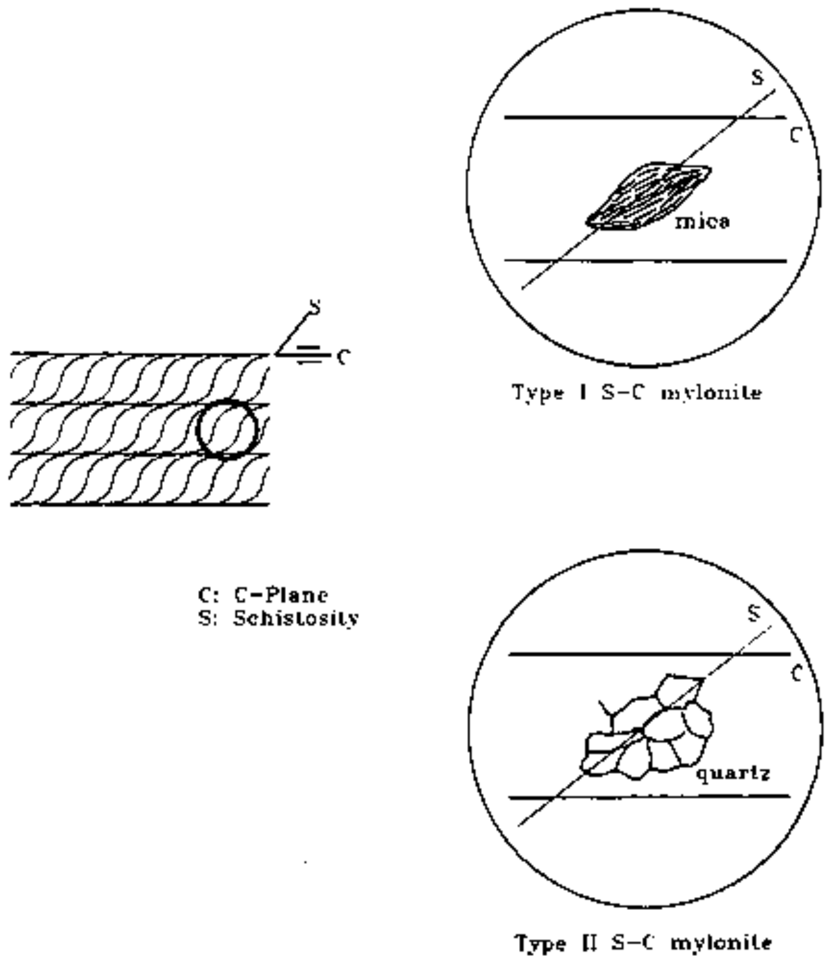

Figure IV-10. Shear sense determination from the orientation relation of S- and C- planes. See text for details.

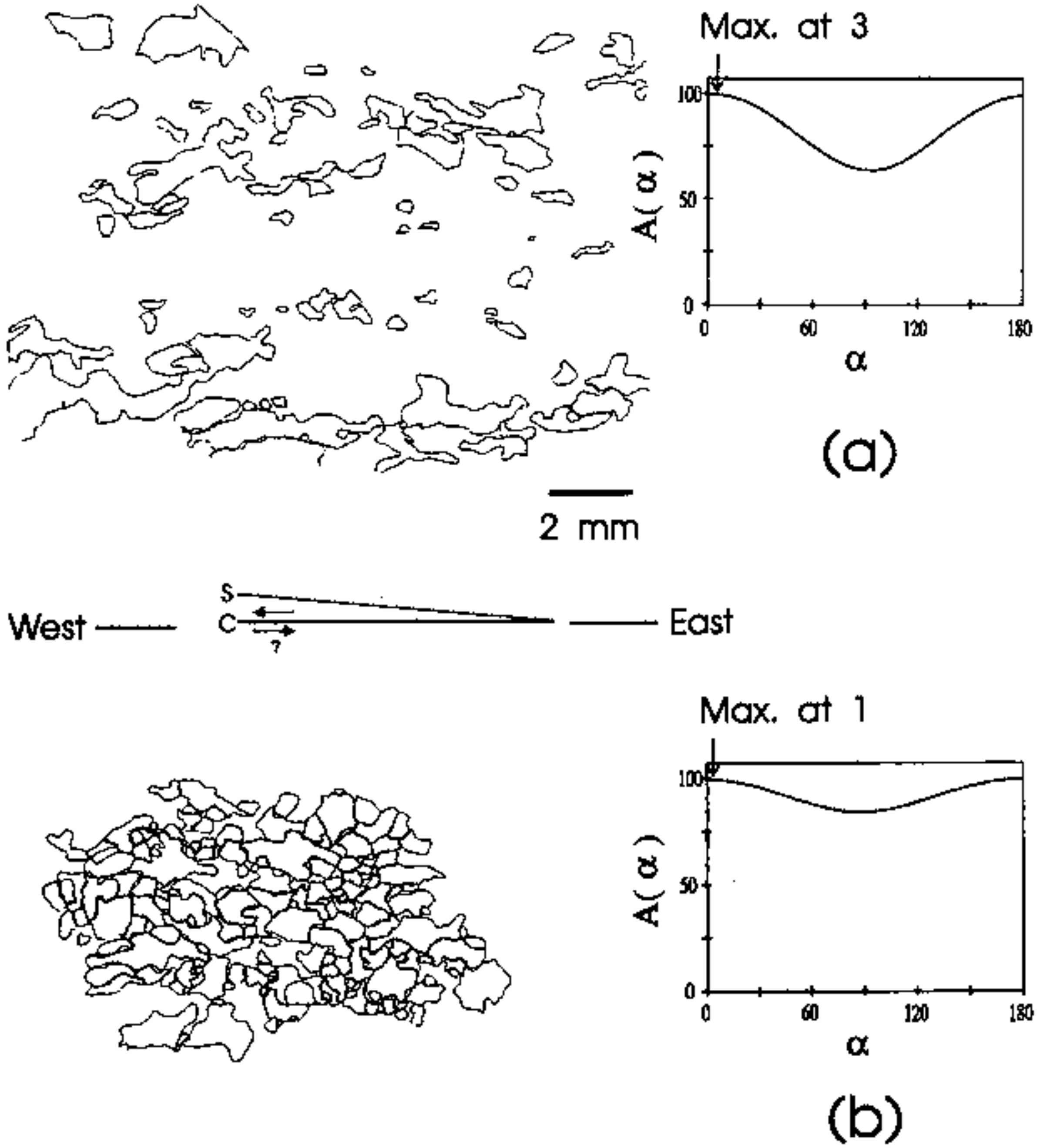

Figure IV-11. Traced grain boundaries and "GBO" output. (a) C-fabric defined by mafic minerals. (b) C- and S- fabric cross cutting relationship. Figure (a) is the traced grain boundary of mafic minerals and Figure (b) is the traced grain boundary of quartz and feldspar. Figures (a) and (b) are from the same thin section.

Figure IV-12 is the digitized image of quartz ribbon grain boundaries and "GBO" output with the C-fabric oriented parallel to the long edge of the reference rectangles. Four samples (88-9, 88-15G, 88-20, and 88-47) seem to show hanging wall to the west sense of shear and one sample (88-36) shows hanging wall to the east sense of shear. The rest of the samples (88-40 and 88-32) show symmetrical grain boundary orientation relative to the C-fabric.

Although the results from "GBO" are not unequivocal, it should be emphasized that this technique would give better results for rocks of low strain, since there is larger angle difference between S- and C- fabric in low-strained rocks.

Shear sense from an outcrop fold

Along the amphibolite and the granitic gneiss lithologic boundary is found folded amphibolite (Figure IV-3). Assuming this fold is formed by non-coaxial deformation, the shear sense is hanging wall to the west. The assumption about the non-coaxial deformation seems to be reasonable since the granitic gneiss would have been folded and found under the amphibolite if the folding was formed by buckling.

Discussion

Except the shear sense from the outcrop scale folding, the shear sense from the microfabric (c-axis pattern and shape fabric orientation) is only slightly hanging wall to the west dominant. The word "slightly" is used since the structural pattern

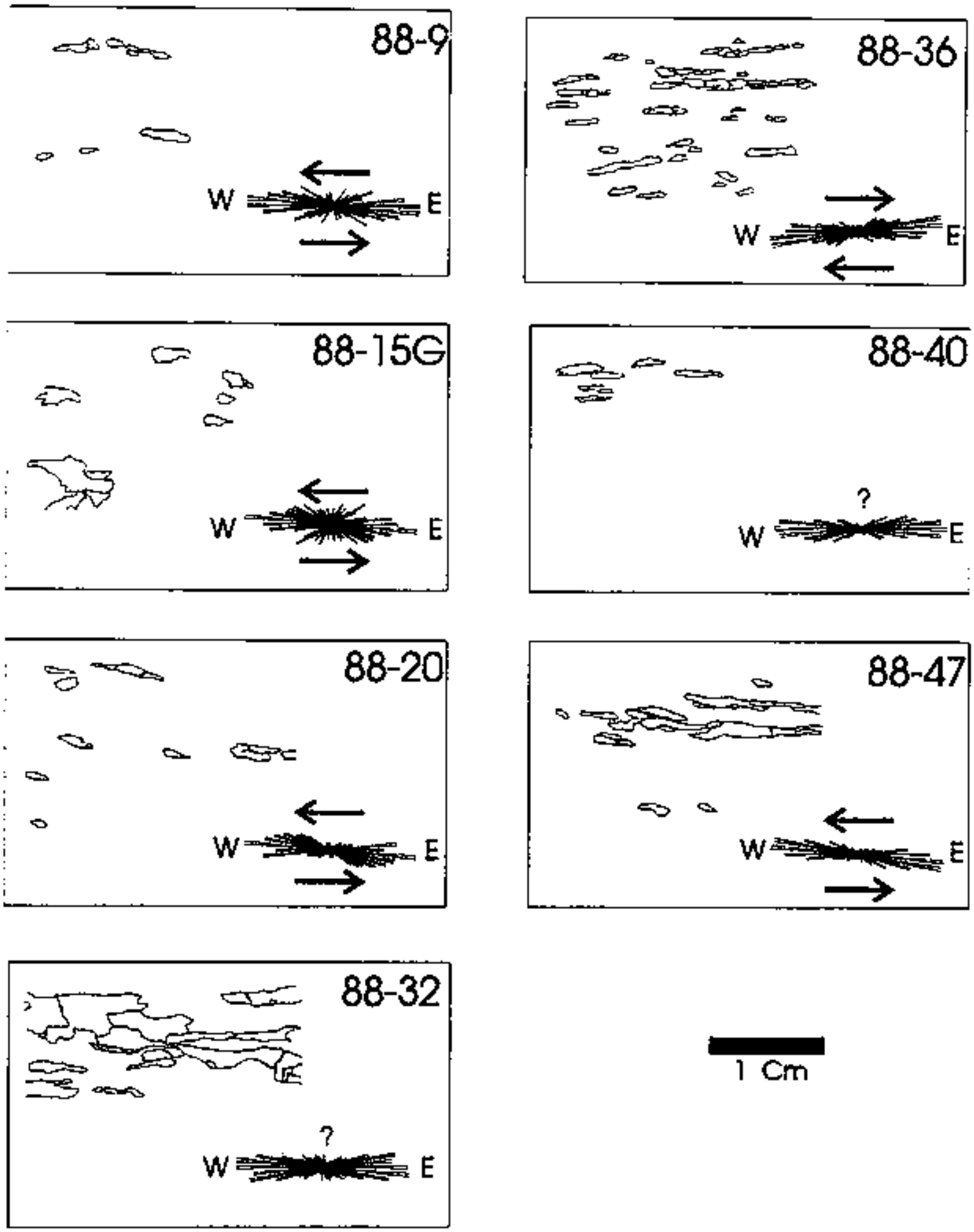

Figure IV-12. Traced quartz ribbon boundaries and "GBO" output.

is close to being symmetric. There are two possible explanations for the symmetry. First, the nature of deformation could be very close to coaxial deformation. As discussed, in the case of a kinematic vorticity number close to zero (e.g. 0.2), the pattern of structural elements can be symmetric. Second, an intense deformation can also produce a symmetric pattern in the structural elements. For example, the S-fabric approaches an orientation parallel to the C-fabric as the strain accumulates.

V. TIMING OF SHEAR ZONE DEFORMATION

The Ar isotope mineral dating technique can give the timing of the cooling through the blocking temperature of a certain mineral and be used to construct the cooling path and uplift history of a region. Dating the deformation events, however, is difficult because there is almost no relation between deformation and isotopic change. In this chapter, an indirect way of dating a deformation is discussed using the temperature condition for certain microstructures found in minerals.

It is possible to infer the approximate temperature range of deformation using the plastic deformation microstructures because certain temperature conditions are necessary to form certain deformation-related microstructures. I will call these microstructures "microstructural geothermometers" because it is possible to estimate the temperature of deformation with these plastic deformation microstructures. Some of the microstructural thermometers used in this study are from natural rocks (Bell and Etheridge, 1976; Miller and Christie, 1981), and some are from experiments (Tullis and Yund, 1985, 1987; Schmid and others, 1987). Examples of microstructural thermometers from natural rocks (Bell and Etheridge, 1976; Miller and Christie, 1981) are based on the comparison of observed plastic deformation microstructures with a known metamorphic grade (i.e., temperature). Microstructural thermometers from experimental studies (Tullis and Yund, 1985, 1987; Schmid and others, 1987) are from the observed microstructures of different temperature conditions of experiments.

Assuming the microstructural geothermometers give a reasonable range of deformation temperature, it is possible to date the deformation event by imposing mineral deformation conditions onto the cooling history curve of a region. In this study, a simple cooling history curve which excludes the possibility of reheating during cooling, from the Lake George area (Ree, 1991), is used (Figure V-1 (a)). Plastic deformation microstructures from quartz, feldspar and calcite (summarized in Figure V-1 (b)) are carefully examined under the petrographic microscope to impose the deformation event on the cooling history curve.

Figure V-1 (a) is the cooling history of the Lake George area. The Lake George area is located about 40 km. to the southeast of the field area. Using the general temperature conditions, the metamorphic grade windows are drawn (Figure V-2) since the microstructural geothermometers (plastic deformation features of minerals) give an approximate range of temperature conditions in terms of metamorphic facies rather than exact temperature conditions.

Three alternative temperature conditions for the feldspar-microstructural geothermometer are placed on the cooling history curve: (i) cataclastic flow regime (Figure V-3 (a)), (ii) dislocation creep regime (Figure V-3 (b)), and (iii) cataclastic flow after dislocation creep regime (Figure V-3 (c)). The feldspar cataclastic flow regime model is valid if neighboring feldspar grains are from different parent grains, which may result in different geochemistry between neighboring grains. The feldspar ductile deformation regime is also possible since slight rotation after dynamic recrystallization can produce apparently different-looking feldspar grains (compare Figure V-3 with Figure IV-7).

Quartz ribbons show subgrain boundaries perpendicular to the foliation and lineation, suggesting dominant basal slip. This microstructure is interpreted to be formed at temperature conditions lower than the temperature of lower amphibolite facies metamorphism (Bell and Etheridge, 1976; Miller and Christie, 1981). The

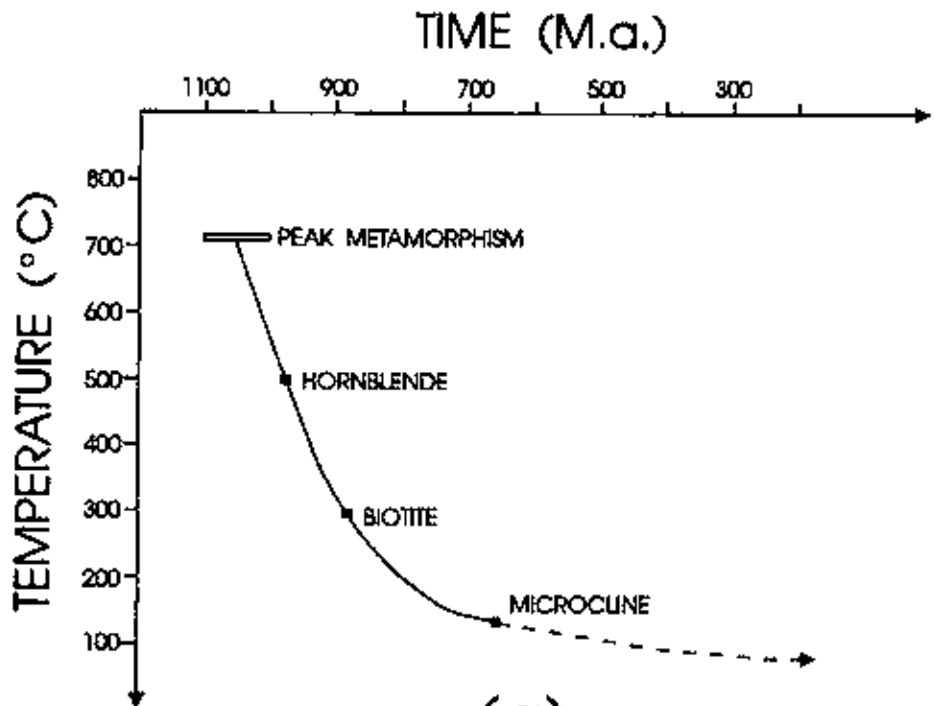

(a)

MINERAL / TEMPERATURE	QUARTZ	FELDSPAR	CALCITE
GRANULITE FACIES METAMORPHISM	?	SUBGRAIN BOUNDARY DYNAMIC RECRYSTALLIZATION (TULLIS AND YUND, 1987)	?
AMPHIBOLITE FACIES METAMORPHISM	PREFERRED ORIENTATION BY PRISMATIC SLIP (BELL AND ETHERIDGE, 1976)		GRAIN BOUNDARY MIGRATION GRAIN BOUNDARY SLIDING
GREENSCHIST FACIES METAMORPHISM	PREFERRED ORIENTATION BY BASAL SLIP (MILLER AND CHRISTIE, 1981)	GRAIN SCALE FAULTS (TULLIS AND YUND, 1987) (TULLIS AND YUND, 1985)	INTRACRYSTALLINE SLIP (SCHMID AND OTHERS, 1987) TWINNING (SCHMID AND OTHERS, 1987)

(b)

Figure V-1. Diagram illustrating the possibility to determine the timing of the ductile shear zone deformation using the cooling history and "microstructural geothermometers". (a) Cooling history of the Lake George area by $^{40}Ar/^{39}Ar$ mineral dates (Ree, 1991). The Lake George area is located about 40 Km to the southeast from the study area. (b) Deformation related microstructures for quartz, feldspar and calcite at different temperature conditions.

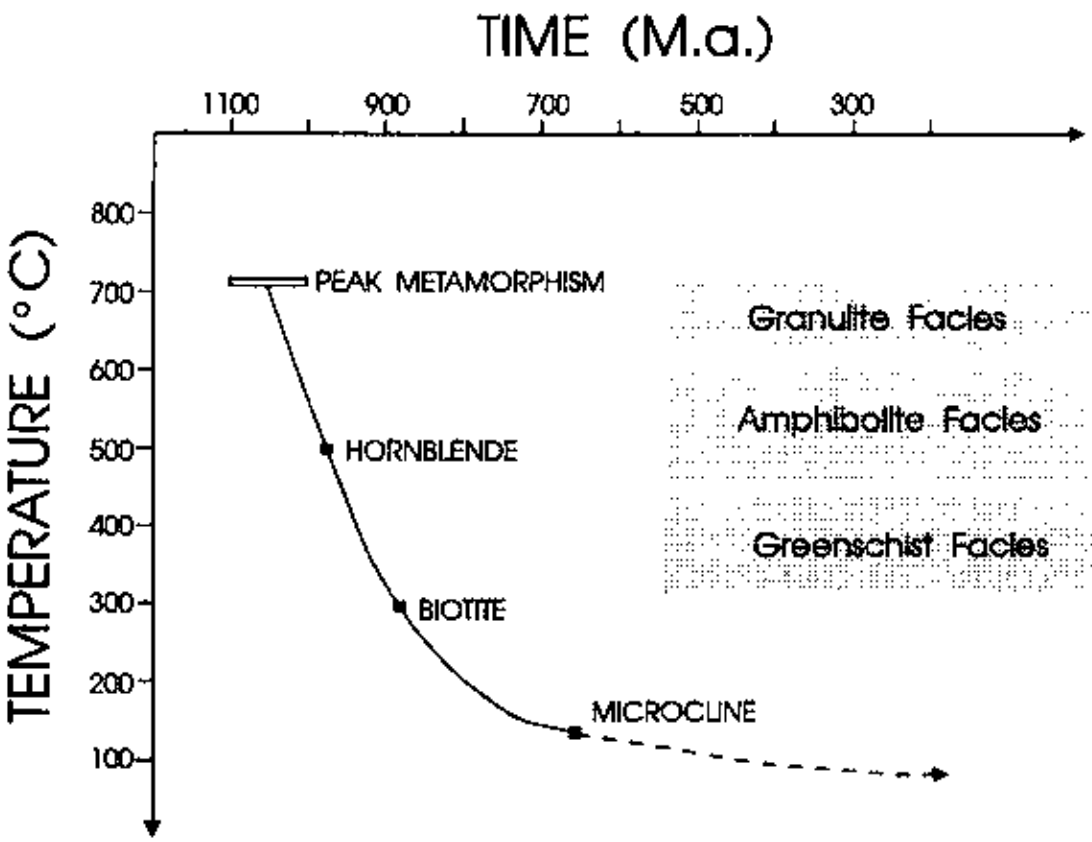

Figure V-2. Cooling history of the Lake George area (Ree, 1991). The metamorphic facies windows are drawn after the P-T diagram in Best (1982).

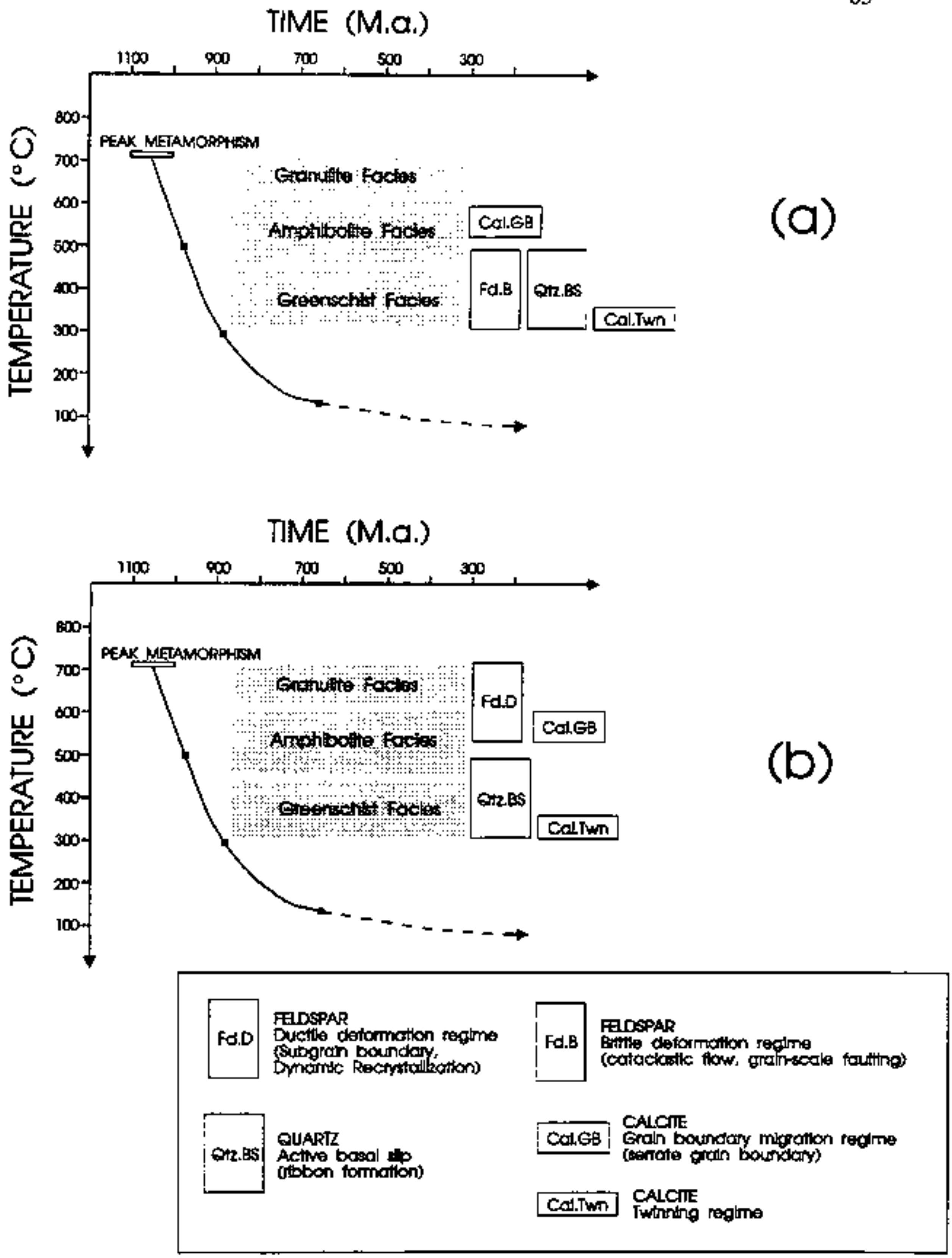
TIME (M.a.)
1100
900
700
500
300
TEMPERATURE (°C)
800
700
600
500
400
300
200
100
PEAK METAMORPHISM
Granulite Facies
Amphibolite Facies
Greenschist Facies
Cal.GB
Fd.B
Qtz.BS
Cal.Twn
(a)
TIME (M.a.)
1100
900
700
500
300
TEMPERATURE (°C)
800
700
600
500
400
300
200
100
PEAK METAMORPHISM
Granulite Facies
Amphibolite Facies
Greenschist Facies
Fd.D
Cal.GB
Qtz.BS
Cal.Twn
(b)
Fd.D
FELDSPAR
Ductile deformation regime
(Subgrain boundary,
Dynamic Recrystallization)
Fd.B
FELDSPAR
Brittle deformation regime
(cataclastic flow, grain-scale faulting)
Qtz.BS
QUARTZ
Active basal slip
(ribbon formation)
Cal.GB
CALCITE
Grain boundary migration regime
(serrate grain boundary)
Cal.Twn
CALCITE
Twinning regime

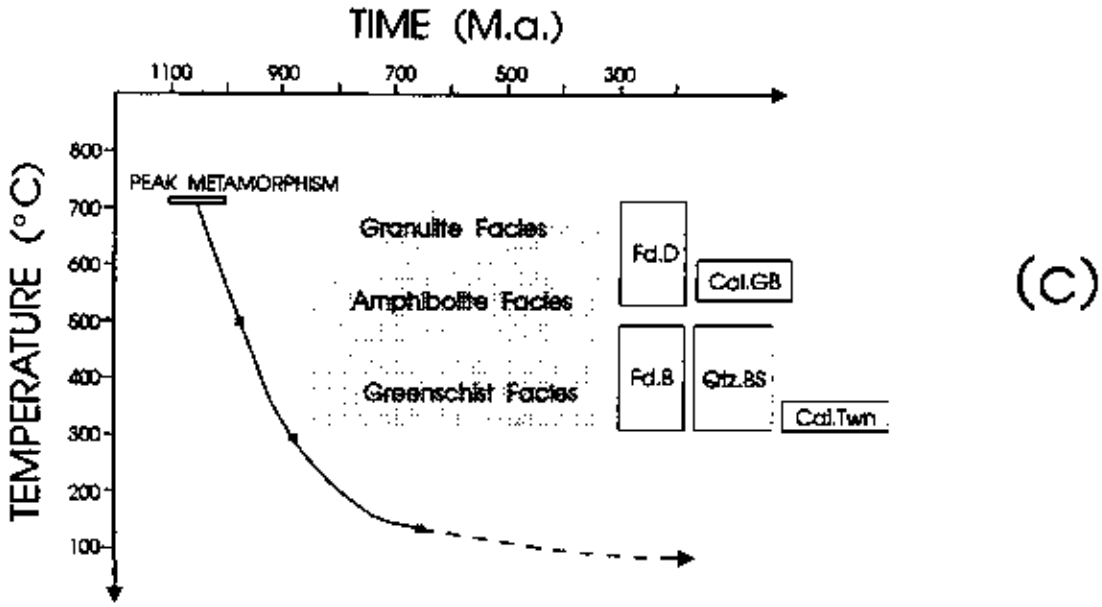

Figure V-3. Three possible models for the timing of ductile shear zone deformation, if the small grain size of feldspar is interpreted as formed by (a) cataclastic flow, (b) extensive recrystallization, and (c) cataclastic flow after extensive recrystallization.

higher temperature slip system texture, which is prismatic slip, seems to be annealed.

Calcite in the marble shows two different deformation regime microstructures: (i) twinning regime and (ii) grain boundary migration regime. The temperature boundary between these two microstructures is around lower greenschist facies metamorphism (Schmid and others, 1987).

Microstructural thermometers from feldspar (of three alternative models), quartz, and calcite are placed on Figure V-2. It is shown in Figure V-3 that the ductile shear zone deformation began on early stage of cooling after peak metamorphism and persisted in this area for at least 150 m.y..

VI. DISCUSSION

In this chapter, three problems concerning dating the deformation, the nature of shear zone deformation, and the determined shear sense will be discussed.

In dating the deformation, the following assumptions were made: (i) there was no reheating during cooling and (ii) referenced microstructural geothermometers are reliable. The first assumption about no reheating can cause significant error in dating the deformation. For example, the duration of shear zone deformation can be a lot shorter if the temperature goes down to greenschist facies metamorphism during the first 50 million years after the peak metamorphism and goes up to the hornblende blocking temperature again as plotted. Therefore, it is necessary to examine the metamorphic textures formed by reheating (prograde metamorphism). The second assumption about the temperature range indicated by the deformation microstructure is also questionable. Microstructural geothermometers from experiments (e.g. Tullis and Yund, 1985) can mislead since extrapolations from laboratory conditions to natural conditions can be erroneous because of huge strain rate differences between laboratory conditions ($\sim 10^{-4}$/sec) and natural conditions ($\sim 10^{-14}$/sec).

Another problem is the nature of the shear zone deformation. The estimated duration of shear zone deformation in this study, based on several assumptions, is 150 to 200 million years. It is worthwhile to consider the nature of the deformation during this time interval: Was the deformation continuous over a wide range of time and temperature? Or was it a series of punctuated events? Maybe the only way to answer these questions is to carefully examine the deformation microstructures of two coexisting phases, e.g., feldspar and quartz, a problem which has just started to attract the attention of experimental structural geologists. This problem will remain unsolved until satisfactory experimental results are achieved.

The shear sense determined from quartz c-axis fabric and the cross cutting relationship between S- and C- fabric is slightly hanging-wall-to-the-west dominant. However, close examination reveals that these microstructures are more symmetric than asymmetric. As discussed in Chapter IV, symmetry in structural elements can be produced by intense shear zone deformation or almost coaxial flow with a small non-coaxial component.

VII. SUMMARY

1. Strong subhorizontal foliation and east-west trending lineations with plastic deformation microstructures suggest subhorizontal ductile shear zone deformation at Oliver and Snyder Hills, Minerva, southeastern Adirondacks.

2. The shear sense determined from various indicators is slightly hanging-wall-to-the-west dominant. However, structural elements such as c-axis fabric of quartz and the S- and C- fabric cross-cutting relationship show more symmetry than asymmetry. The symmetry in these structural elements can be interpreted as formed by intense deformation or almost coaxial deformation.

3. It is possible to estimate the timing of shear zone deformation using the regional cooling history curve and microstructural geothermometers. The time relationship shows that the ductile shear zone deformation was present over a wide period of time and temperature.

References

Bailey, E.H. and Stevens, R.E., 1960, Selective staining of K-feldspar and plagioclase on rock slabs and thin sections, American Mineralogist, **45**, pp. 1020-1025

Beach, A., 1980, Retrogressive metamorphic processes in shear zones with special reference to the Lewisian complex, Journal of Structural Geology, 2, pp. 257-263

Bell, T.H. and Etheridge, M.A., 1973, Microstructures of mylonites and their descriptive terminology, Lithos, **6**, pp. 337-348

Bell, T.H. and Etheridge, M.A., 1976, The deformation and recrystallization of quartz in a mylonite zone, Central Australia, Tectonophysics, **32**, pp. 235-267

Berthe, D., Choukroune, P. and Jegouzo, P., 1979, Orthogneiss, mylonite and non coaxial deformation of granites: the example of the South Amorican Shear Zone, Journal of Structural Geology, 1, pp. 31-42

Best, M.G., 1982, Igneous and metamorphic petrology, W.H. Freeman and Company, 630p.

Bohlen, S.R. and Mezger, K., 1989, Origin of granulite terranes and the formation of the lowermost continental crust, Science, **244**, pp. 326-329

De Waard, D., 1965, A proposed subdivision of the granulite facies, American Journal of Science, **263**, pp. 455-461

Emslie, R.F., 1978, Anorthosite massifs, rapakivi granites, and late Proterozoic rifting of North America, Precambrian Research, 7, pp. 61-98

Etchecopar, A., 1977, A plane kinematic model of progressive deformation in a polycrystalline aggregate, Tectonophysics, **39**, pp. 121-139

Hobbs, B.E., Means, W.D. and Williams, P.F., 1976, An outline of structural geology, John Wiley & Sons, Inc., 571p.

Isachsen, Y.W. and Fisher, D.W., 1970, Geologic Map of New York: Adirondack sheet, New York State Geological Survey

Ji, S. and Mainprice, D., 1990, Recrystallization and fabric development in plagioclase, Journal of Geology, **98**, pp. 65-79

Lister, G.S. and Snoke, A.W., 1984, S-C Mylonites, Journal of Structural Geology, **6**, pp. 617-638

Lonker, S., 1980, Conditions of metamorphism in high-grade pelitic gneisses from the Frontenac Axis, Ontario, Canada, Canadian Journal of Earth Science, 17, pp. 1666-1684

Means, W.D., 1990, Kinematics, stress, deformation and material behavior, Journal of Structural Geology, 12, pp. 953-971

Miller, D.M. and Christie, J.M., 1981, Comparison of quartz microfabric with strain in recrystallized quartzite, Journal of Structural Geology, **3**, pp. 129-141

Nicolas, A., 1986, Principles of rock deformation, Reidel Publishing Company, 208p.

Nockolds, S.R., Knox, R.W.O. and Chinner, G.A., 1978, Petrology, Cambridge University Press, 435p.

Panozzo, R., 1983, Two-dimensional analysis of shape fabric using projections of lines in a plane, Tectonophysics, **95**, pp.279-294

Passchier, C.W., 1987, Stable positions of rigid objects in non-coaxial flow - a study in vorticity analysis, Journal of Structural Geology, 9, pp. 679-690

Poirier, J.-P., 1985, Creep of crystals, University of Cambridge Press, 260p.

Ramsay, J.G., 1980, Shear zone geometry: a review, Journal of Structural Geology, **2**, pp. 83-99

Ramsay, J.G. and Huber, M.I., 1983, The techniques of modern structural geology, Academic Press, **1**., 307p.

Ree, B.-N., 1991, Mineral paragenesis of the granulite facies in the Lake George area, New York, unpublished SUNY-Albany M.S. thesis, 67p.

Schmid, S.M., Panozzo, R. and Bauer, S., 1987, Simple shear experiments on calcitic rocks: rheology and microfabric, Journal of Structural Geology, **9**, pp. 747-778

Tullis, J. and Yund, R.A., 1985, Dynamic recrystallization of feldspar: A mechanism for ductile shear zone formation, Geology, **13**, pp. 238-241

Tullis, J. and Yund, R.A., 1987, Transition from cataclastic flow to dislocation creep of feldspar: Mechanism and microstructures, Geology, **15**, pp. 606-609

Turner, F.J., 1981, Metamorphic petrology: Mineralogical, Fluid, and Tectonic Aspects (second ed.), Hemisphere Pub. Co., 524p.

van der Plas, L. and Tobi, A.C., 1965, A chart for judging the reliability of point counting results, American Journal of Science, **263**, pp. 87-90

White, S.H., Burrows, S.E., Carreras, J., Shaw, N.D. and Humphreys, F.J., 1980, On mylonites in ductile shear zones, Journal of Structural Geology, **2**, pp. 175-187

Winkler, H.G.F., 1979, Petrogenesis of metamorphic rocks, Springer-Verlag, 348p.

Appendix A. Glossary

Coaxial flow: flow with the stretching directions parallel to the same material lines from one moment to the next (Means, 1990)

Climb (dislocation climb): At high temperature or at slow strain rate deformation, edge dislocations are no longer constrained to remain in their slip plane. By diffusion of material toward or away from the dislocation core, the length of the extra half plane can be altered so that the dislocations climb from one slip plane to the next (Hobbs and others, 1976, p.90).

Dynamic Recrystallization: A process whereby strain-hardened grains are replaced by new unstrained grains.

High angle boundary (grain boundary): planar defect where lattice misorientation is greater than 5 degrees.

Low angle boundary (subgrain boundary): planar defect where lattice misorientation is 1° to 5° (Hobbs and others, 1976, p. 93).

Non-coaxial flow: flow with different material lines parallel to the stretching directions from one moment to the next (Means, 1990)

Recovery: (In broad sense) All the processes that attempt to return a deformed crystal to the undeformed state without the formation and migration of *high angle boundaries*. Most of the recovery processes are associated with a general decrease in the dislocation density resulting from the edge components of dislocations climbing until they meet another dislocation of opposite sign and annihilating each other. The screw components cross slip to produce similar results. Since this process involves *climb*, recovery can only take place at a temperature where solid-state diffusion can proceed at a rate sufficient to produce an appreciable climb rate (Hobbs and others, 1976, p. 108).

Strain Hardening: At low temperature deformation, dislocations moving on the slip plane tend to be obstructed by various obstacles such as other dislocations, impurities, precipitates, and grain boundaries. For deformation to go on, stress increase is needed. This condition on the stress-strain curve for a material is defined as strain hardening (Nicolas, 1986, p. 38).

Strain Softening: An increase in strain rate at constant stress or a reduction in stress at constant strain rate (White and others, 1980).

Appendix B.
Orientation of samples

Sample #	Orientation
88-1	N17E
88-2	N70W
88-3	S43E
88-4	S70E
88-4A	N40W
88-5	N.O.
88-6G	S43W
88-6GL	S40W
88-7	S20W
88-9	N70W
88-10	N25W,48S
88-11	N15W,79S
88-12	N71W
88-13	N10W,84N
88-14	S70E
88-15	S58E
88-15G	S25E
88-16	S10W
88-17	N68W,84S
88-18	S8W
88-19	S10W
88-20	N28E
88-21	N54W
88-23	S12E
88-24	S75W
88-25	S15E
88-26	S75E
88-27	N85E

Sample #	Orientation
88-28	S28E
88-29	S15E
88-30	S78E
88-30A	N82W
88-31	S70E
88-32	S80E
88-33	N
88-34	S62E
88-35	N85W
88-36	S6E
88-37	S70W
88-38	S10W
88-39	N75E
88-40	S78W
88-40-1	N75W
88-41	S15E
88-42	S50W
88-43	N55E
88-44	N65E
88-45	N30W
88-46	S71E
88-47	N38W
88-49	S60E
88-50	N70W
88-52	S75W,65N
89-1	N.O.
89-2	N40E
89-4	N5E,71E

Sample #	Orientation
89-5	W
89-6A	N75W,65S (OVT.)
89-6B	S30W
89-6C	S75E,90
89-6D	N.O.
89-9	N.O.
89-14	N.O.
89-15	N78W,80S
89-19	S15E
89-19-2	N.O.
89-21	N.O.
89-23	N50E
89-24	N.O.
89-26	N30W
89-27	N80E
89-28	S75E
89-29	S75E
89-29-2	S50E
89-30	N75E
89-31	N,5(L.)
89-32	N30E
89-33	N52E
89-34	E,15(L.)
89-35	N.O.

N.O. = Not Oriented
OVT. = Overturned Plane

L. = Lineation

Samples with TREND only, have two horizontal lines, and the drawn arrow is the trend of one of the two lines.

STRIKE & DIP represent the orientation of marked surface.

APPENDIX C. Source code of the Program "GBO"

The program "GBO" is coded in Microsoft QuickBasic (version 4.5) and composed of 7 programs and 1 MS-DOS batch file which automatically executes the program in order. The seven programs are "GBO_STRT", "GBO_CNV", "GBO_ALP", "GBO_MAIN", "GBO_ROSE", "GBO_SCR", and "GBO_ACS1". The batch file is "GBO.BAT". The functions of each individual program are explained in the PRINT statement of the program "GBO_STRT". Sections C.1 to C.8 are the source code of the batch file and programs.

C.1. GBO.BAT

```
dir *.scr /w
dir *.dxf /w
pause
echo off
gbo_strt
gbo_cnv
gbo_alp
gbo_main
gbo_rose
gbo_scr
gbo_acsl
```

C.2. GBO_STRT

```
FOR i = 1 TO 25: PRINT : NEXT i
PRINT "                                          ==========="
PRINT "                                          Program GBO"
PRINT "                                          ==========="
PRINT "                                                     Ver. 1.1"
PRINT "                                                     Jan. 12, 1990"
PRINT "               by Jin-Han Ree, Dept. of Geological Sci., SUNY at
Albany"
PRINT "                & Youngdo Park, Detp. of Geology, Temple Univ."
PRINT
PRINT
PRINT
PRINT
PRINT
PRINT "                   This progam calculates the orientation"
PRINT "                  of foliation (referred as â:angle from"
PRINT "                  positive x-axis) USING THE GRAIN       "
PRINT "                  BOUNDARY ORIENTATION.                  "
PRINT
PRINT
PRINT
PRINT
PRINT
PRINT
PRINT
PRINT "                        Press any key to continue......";
DO
LOOP UNTIL INKEY$ <> ""
PRINT "                                          ==========="
PRINT "                                          Restriction"
PRINT "                                          ==========="
PRINT
PRINT "                      The Maximum number of data points"
PRINT "                      for 640K system is 7000 which is"
PRINT "                      about 390K bytes in DXF file."
PRINT
PRINT
PRINT
PRINT "                                             ====="
PRINT "                                             Speed"
PRINT "                                             ====="
PRINT
PRINT "                      It took about 60 minutes to calcuate "
PRINT "                      3000 DATA points on 10MHz 80286 machine."
PRINT "                      * 20 minutes on 10MHz 80287 coprocessor"
FOR i = 1 TO 6: PRINT : NEXT i
PRINT "                        Press any key to continue......";
DO
LOOP UNTIL INKEY$ <> ""
PRINT "                                  ==================="
PRINT "                                  Data Processing Flow"
PRINT "                                  ==================="
PRINT
PRINT "              *  GBO_STRT.EXE prints the information and records"
PRINT "                               the FILENAME data to GBO.CFG file"
PRINT "              *  GBO_CNV.EXE  extracts XY coordinate of point"
PRINT "                               from DXF (AutoCad) file and writes
TMP"
PRINT "                               file."
PRINT "              *  GBO_ALP.EXE  calculates the Length & Slope of"
PRINT "                               a line which is defined by two
close"
PRINT "                               points and writes ALP file."
PRINT "              *  GBO_MAIN.EXE calculates A(â) and writes DAT"
PRINT "                               file. *See Schmidt, 1987*"
PRINT "              *  GBO_ROSE.EXE writes ROSE Diagram SCR (AutoCad)
file."
PRINT "              *  GBO_SCR.EXE  writes A(â) & â SCR file(AutoCad)
file."
PRINT
PRINT
PRINT "                                 * Schmidt,S.M., Panozzo,R. and
Bauer,S., 1987,"
```

```
PRINT "                              Simple shear experiments on calcite
rocks:"
PRINT "                              rheology and microfabric, J. of
Structural"
PRINT "                              Geology, Vol. 9, pp 747-778."
PRINT
PRINT "                         Press any key to continue......";
DO
LOOP UNTIL INKEY$ <> ""
FOR i = 1 TO 25: PRINT : NEXT i
PRINT "-------------------"
PRINT "Do not type '.DXF'."
PRINT "==================="
INPUT "DXF filename"; a$
OPEN "GBO.CFG" FOR OUTPUT AS #1
PRINT #1, a$
PRINT #1,
CLOSE #1
END
```

C.3. GBO_CNV

```
DECLARE SUB OpenDxf ()
DECLARE SUB Pass (cnt!, a$)

COMMON SHARED cnt
COMMON SHARED a$

CALL OpenDxf

DO
  CALL Pass(1, a$)
LOOP UNTIL a$ = "POLYLINE"

CALL Pass(12, a$)
DO
  PRINT #2, "POLYLINE"
  DO
    CALL Pass(3, a$)
    INPUT #1, x
    CALL Pass(1, a$)
    INPUT #1, y
    CALL Pass(4, a$)
    PRINT #2, "***"
    PRINT #2, USING "####.######"; x;
    PRINT #2, ",";
    PRINT #2, USING "####.######"; y
  LOOP UNTIL a$ = "SEQEND"
  PRINT #2, "SEQEND"
  CALL Pass(4, a$)
  IF a$ = "POLYLINE" THEN CALL Pass(12, a$)
LOOP UNTIL a$ = "ENDSEC"

PRINT #2, "ENDSEC"
PRINT #2, "EOF"
CLOSE #1 'input file
CLOSE #2 'output file
END

SUB OpenDxf
  PRINT "Running GBO_CNV.EXE (DXF to TMP conversion)"
  PRINT "-------------------------------------------"
  PRINT "BEGIN AT "; TIME$; "///"; DATE$
  OPEN "gbo.cfg" FOR INPUT AS #1
  INPUT #1, f$
  CLOSE #1
  OPEN f$ + ".dxf" FOR INPUT AS #1
  OPEN f$ + ".tmp" FOR OUTPUT AS #2
END SUB

SUB Pass (cnt, a$)
  'Passing the unnecessary parameters in DXF file
  FOR i = 1 TO cnt
    INPUT #1, a$
  NEXT i
END SUB
```

C.4. GBO_ALP

```
DECLARE SUB OpenTmp (x!, Y!, seqend!, seqcnt!)

CONST MaxArray = 7000
CONST ToDeg = 57.29578#
CONST ToRad = .017453

DIM SHARED x(1 TO MaxArray), Y(1 TO MaxArray)
DIM SHARED seqend(1 TO 500)
COMMON SHARED seqcnt

CALL OpenTmp(x, Y, seqend, seqcnt)

PRINT #2, seqend(seqcnt) - seqcnt + 1

FOR i = 1 TO seqcnt - 1
  FOR j = seqend(i) + 1 TO seqend(i + 1)
    IF j < seqend(i + 1) THEN
      d = SQR((x(j) - x(j + 1)) ^ 2 + (Y(j) - Y(j + 1)) ^ 2)
      xrun = x(j + 1) - x(j)
      IF xrun = 0 THEN
                    alpha = 90
                  ELSE
                    alpha = ATN((Y(j + 1) - Y(j)) / xrun) * ToDeg
                  END IF
      PRINT #2, USING "####.######"; d;
      PRINT #2, ",";
      PRINT #2, USING "#####.######"; alpha
    END IF
  NEXT j
NEXT i
PRINT #2,
CLOSE #2
END
'-----------------------------------------------------------

SUB OpenTmp (x, Y, seqend, seqcnt)
  PRINT "Running GBO_ALP.EXE (TMP to ALP conversion)"
  PRINT "-----------------------------------------"
  OPEN "gbo.cfg" FOR INPUT AS #1
  INPUT #1, f$
  CLOSE #1
  OPEN f$ + ".tmp" FOR INPUT AS #1
  OPEN f$ + ".alp" FOR OUTPUT AS #2
  PRINT "BEGIN AT "; TIME$; "///"; DATE$
  i = 0
  j = 1
  seqend(1) = 0
  INPUT #1, a$: INPUT #1, a$
  DO
    DO
      i = i + 1
      INPUT #1, x(i), Y(i)
      INPUT #1, a$
    LOOP UNTIL a$ = "SEQEND"
    j = j + 1: seqend(j) = i
    INPUT #1, a$
    IF a$ = "POLYLINE" THEN
      INPUT #1, a$
    END IF
  LOOP UNTIL a$ = "ENDSEC"
  seqcnt = j
  CLOSE #1
END SUB
```

C.5. GBO_MAIN

```
DECLARE SUB OpenAlp (d!, alp!, cnt!)
CONST MaxArray = 7000
CONST ToDeg = 57.29578#
CONST ToRad = .017453

DIM SHARED d(1 TO MaxArray), alp(1 TO MaxArray)
DIM rot(0 TO 180)
COMMON SHARED cnt
start = TIMER
CALL OpenAlp(d, alp, cnt)
FOR i = 1 TO 18: PRINT "0123456789"; : NEXT i: PRINT "0"
FOR r = 0 TO 180
  FOR i = 1 TO cnt
    rot(r) = rot(r) + d(i) * ABS(COS(ToRad * (alp(i) - r)))
  NEXT i
  PRINT "0";
NEXT r
PRINT

max = -999

FOR r = 0 TO 180
    IF rot(r) > max THEN max = rot(r)
NEXT r

FOR r = 0 TO 180
  rot(r) = rot(r) / max * 100
  PRINT #2, USING "#####"; r;
  PRINT #2, ",";
  PRINT #2, USING "#####.##"; rot(r)
NEXT r
CLOSE #2
final = TIMER
PRINT " Run Time= "; INT(final - start); " seconds....."
PRINT
END

SUB OpenAlp (d, alp, cnt)
  PRINT "Running GBO_MAIN.EXE (ALP to DAT conversion)"
  PRINT "--------------------------------------------"
  PRINT "BEGIN AT "; TIME$; "///"; DATE$
  OPEN "gbo.cfg" FOR INPUT AS #1
  INPUT #1, f$
  CLOSE #1
  OPEN f$ + ".alp" FOR INPUT AS #1
  OPEN f$ + ".dat" FOR OUTPUT AS #2
  INPUT #1, cnt
  PRINT "Number of Data="; cnt
  FOR i = 1 TO cnt
    INPUT #1, d(i), alp(i)
  NEXT i
  CLOSE #1
END SUB
```

C.6. GBO_ROSE

```
DECLARE SUB pr (x!, y!)

CONST MaxArray = 7000
CONST ToRad = .017453

REM $DYNAMIC

DIM d(1 TO MaxArray), alp(1 TO MaxArray), counter(0 TO 71)

PRINT "Writing Rose Diagram SCR File"
PRINT "============================="
PRINT "BEGIN AT "; TIME$; "///"; DATE$
OPEN "GBO.CFG" FOR INPUT AS #1
INPUT #1, f$
CLOSE #1

OPEN f$ + ".ALP" FOR INPUT AS #1
INPUT #1, cnt
FOR i = 1 TO cnt
  INPUT #1, d(i), alp(i)
  IF alp(i) < 0 THEN alp(i) = 180 + alp(i)
NEXT i
CLOSE #1

FOR i = 0 TO 35: counter(i) = 0: NEXT i

FOR i = 1 TO cnt
  FOR j = 0 TO 35
    a = j * 5 - 2.5
    b = j * 5 + 2.5
    IF (alp(i) >= a) AND (alp(i) < b) THEN
      counter(j) = counter(j) + d(i)
      GOTO 1
    END IF
  NEXT j
1
NEXT i

max = -999
FOR i = 0 TO 35
  IF counter(i) > max THEN max = counter(i)
NEXT i

radius = 2.75: cx = 12: cy = 2.75
FOR i = 0 TO 35: counter(i) = radius * counter(i) / max: NEXT i

FOR i = 36 TO 71: counter(i) = counter(i - 36): NEXT i

OPEN f$ + ".scr" FOR OUTPUT AS #1
PRINT #1, "zoom"
PRINT #1, "0.8"
PRINT #1,
PRINT #1,
FOR i = 0 TO 71
    a = (i * 5) * ToRad
    r = counter(i)
    IF r < .1 THEN GOTO 2
    x1 = r * COS(a) + cx: y1 = r * SIN(a) + cy
    PRINT #1, "pline"
    CALL pr(cx, cy)
    PRINT #1, "width"
    PRINT #1, "0.01"
    PRINT #1, "0.01"
    CALL pr(x1, y1)
    PRINT #1,
2
NEXT i
PRINT #1, "text"
PRINT #1, "middle"
PRINT #1, "15.5,2.75"
PRINT #1, "0.2"
PRINT #1, "0"
PRINT #1, "- 0"
PRINT #1, "text"
```

```
PRINT #1, "middle"
PRINT #1, "8.5,2.75"
PRINT #1, "0.2"
PRINT #1, "0"
PRINT #1, "180 -"
PRINT #1, "text"
PRINT #1, "middle"
PRINT #1, "12,6.75"
PRINT #1, "0.2"
PRINT #1, "0"
PRINT #1, "90"
PRINT #1, "circle"
CALL pr(cx, cy)
PRINT #1, "2.75"
PRINT #1, "circle"
CALL pr(cx, cy)
PRINT #1, "1.375"
CLOSE #1

END

SUB pr (x, y)
  d1$ = "#.######": d2$ = "##.######"
  IF x >= 10 THEN
      PRINT #1, USING d2$; x;
    ELSE
      PRINT #1, USING d1$; x;
  END IF
  PRINT #1, ",";
  IF y >= 10 THEN
      PRINT #1, USING d2$; y
    ELSE
      PRINT #1, USING d1$; y
  END IF
END SUB
```

C.7. GBO_SCR

```
PRINT "Writing A & A(&) SCR file"
PRINT "-------------------------"
PRINT "BEGIN AT "; TIME$; "///"; DATE$
OPEN "gbo.cfg" FOR INPUT AS #1
INPUT #1, f$
CLOSE #1
OPEN f$ + ".SCR" FOR APPEND AS #1
OPEN f$ + ".DAT" FOR INPUT AS #2
PRINT #1, "LINE"
PRINT #1, "1,1"
PRINT #1, "1,5.3"
PRINT #1, "7,5.3"
PRINT #1, "7,1"
PRINT #1, "1,1"
PRINT #1, ""
PRINT #1, "LINE"
PRINT #1, "1,0.9"
PRINT #1, "1,1"
PRINT #1, ""
PRINT #1, "LINE"
PRINT #1, "2,0.9"
PRINT #1, "2,1.1"
PRINT #1, ""
PRINT #1, "LINE"
PRINT #1, "3,0.9"
PRINT #1, "3,1.1"
PRINT #1, ""
PRINT #1, "LINE"
PRINT #1, "4,0.9"
PRINT #1, "4,1.1"
PRINT #1, ""
PRINT #1, "LINE"
PRINT #1, "5,0.9"
PRINT #1, "5,1.1"
PRINT #1, ""
PRINT #1, "LINE"
PRINT #1, "6,0.9"
PRINT #1, "6,1.1"
PRINT #1, ""
PRINT #1, "LINE"
PRINT #1, "7,0.9"
PRINT #1, "7,1"
PRINT #1, ""
PRINT #1, "LINE"
PRINT #1, "0.9,1"
PRINT #1, "1,1"
PRINT #2, ""
PRINT #1, "LINE"
PRINT #1, "0.9,2"
PRINT #1, "1.1,2"
PRINT #1, ""
PRINT #1, "LINE"
PRINT #1, "0.9,3"
PRINT #1, "1.1,3"
PRINT #1, ""
PRINT #1, "LINE"
PRINT #1, "0.9,4"
PRINT #1, "1.1,4"
PRINT #1, ""
PRINT #1, "LINE"
PRINT #1, "0.9,5"
PRINT #1, "1.1,5"
PRINT #1, ""
PRINT #1, "TEXT"
PRINT #1, "MIDDLE"
PRINT #1, "1,0.7"
PRINT #1, "0.2"
PRINT #1, "0"
PRINT #1, "0"
PRINT #1, "TEXT"
PRINT #1, "MIDDLE"
PRINT #1, "2,0.7"
PRINT #1, "0.2"
PRINT #1, "0"
```

```
PRINT #1, "30"
PRINT #1, "TEXT"
PRINT #1, "MIDDLE"
PRINT #1, "3,0.7"
PRINT #1, "0.2"
PRINT #1, "0"
PRINT #1, "60"
PRINT #1, "TEXT"
PRINT #1, "MIDDLE"
PRINT #1, "4,0.7"
PRINT #1, "0.2"
PRINT #1, "0"
PRINT #1, "90"
PRINT #1, "TEXT"
PRINT #1, "MIDDLE"
PRINT #1, "5,0.7"
PRINT #1, "0.2"
PRINT #1, "0"
PRINT #1, "120"
PRINT #1, "TEXT"
PRINT #1, "MIDDLE"
PRINT #1, "6,0.7"
PRINT #1, "0.2"
PRINT #1, "0"
PRINT #1, "150"
PRINT #1, "TEXT"
PRINT #1, "MIDDLE"
PRINT #1, "7,0.7"
PRINT #1, "0.2"
PRINT #1, "0"
PRINT #1, "180"
PRINT #1, "TEXT"
PRINT #1, "MIDDLE"
PRINT #1, "4,0.3"
PRINT #1, "0.3"
PRINT #1, "0"
PRINT #1, "ALPHA (DEGREE)"
PRINT #1, "TEXT"
PRINT #1, "MIDDLE"
PRINT #1, "0.7,1"
PRINT #1, "0.2"
PRINT #1, "0"
PRINT #1, "0"
PRINT #1, "TEXT"
PRINT #1, "MIDDLE"
PRINT #1, "0.7,2"
PRINT #1, "0.2"
PRINT #1, "0"
PRINT #1, "25"
PRINT #1, "TEXT"
PRINT #1, "MIDDLE"
PRINT #1, "0.7,3"
PRINT #1, "0.2"
PRINT #1, "0"
PRINT #1, "50"
PRINT #1, "TEXT"
PRINT #1, "MIDDLE"
PRINT #1, "0.7,4"
PRINT #1, "0.2"
PRINT #1, "0"
PRINT #1, "75"
PRINT #1, "TEXT"
PRINT #1, "MIDDLE"
PRINT #1, "0.7,5"
PRINT #1, "0.2"
PRINT #1, "0"
PRINT #1, "100"
PRINT #1, "TEXT"
PRINT #1, "MIDDLE"
PRINT #1, "0.3,3"
PRINT #1, "0.3"
PRINT #1, "90"
PRINT #1, "A(ALPHA)"
PRINT #1, "LINE"
FOR I = 0 TO 180
  INPUT #2, X, Y
  X = X / 30 + 1
  Y = Y / 25 + 1
  PRINT #1, USING "#.###": X;
```

```
  PRINT #1, ",";
  PRINT #1, USING "#.###"; Y
NEXT I
PRINT #1, ""
PRINT #1, "REGEN"
CLOSE #1
CLOSE #2
```

C.8. GBO_ACS1

```
PRINT "PROGRAM GBO_ACS1"
PRINT "================"
PRINT
PRINT
PRINT "Accessory Program for GBO"
PRINT "========================="
PRINT "To get total sum of digitized LINE length"
PRINT
PRINT
PRINT
PRINT "*** Do not type .alp"

INPUT "Name of '.alp' file to read"; f$

OPEN f$ + ".alp" FOR INPUT AS #1
OPEN f$ + ".ac1" FOR OUTPUT AS #2

INPUT #1, count
sum = 0
FOR i = 1 TO count
  INPUT #1, d, a
  sum = sum + d
NEXT i
PRINT sum
PRINT #2, "Total line length for "; f$; " = "; sum

CLOSE #1
CLOSE #2
END
```